

Review

Designing resilient hydrogels: Strategies for minimizing hysteresis while maximizing toughness

Shaowei Han,^{1,2,3} Linlong Xing,^{1,2,3} Yongxin Qin,^{2,3,*} and Caofeng Pan^{1,2,3,*}¹School of Physics, Beihang University, Beijing 100191, China²Institute of Atomic Manufacturing, Beihang University, Beijing 100191, China³International Research Institute for Multidisciplinary Science, Beihang University, Beijing 100191, China*Correspondence: qinyongxin@buaa.edu.cn (Y.Q.), pancaofeng@buaa.edu.cn (C.P.)<https://doi.org/10.1016/j.matt.2025.102489>

PROGRESS AND POTENTIAL Hydrogels have demonstrated considerable potential in flexible electronics and biomedical devices, yet their practical implementation has been constrained by an inherent trade-off: high toughness is often accompanied by substantial energy dissipation (hysteresis), resulting in fatigue and eventual failure over time. This review delineates innovative strategies (such as optimizing network architectures, incorporating dynamic crosslinks, reinforcing with nanomaterials, and designing higher-order structures) that effectively mitigate this challenge. These methodologies enable hydrogels to achieve both high toughness and low hysteresis concurrently, thereby enhancing their reliability for prolonged applications.

Beyond addressing the toughness-hysteresis trade-off, the long-term objectives extend further. The overarching aim is to integrate these four strategies for multiscale design optimization, leverage artificial intelligence for expedited property tuning, and enhance material durability under extreme conditions (such as sub-zero temperatures or arid environments). This research holds both immediate and enduring societal implications. In the near term, these advancements will improve wearable health sensors, facilitating precise monitoring of vital signs, muscle activity, and subtle physiological cues like facial expressions while maintaining long-term accuracy. They will also render implantable devices (such as cardiac signal monitors) safer and more durable, minimizing tissue irritation and mechanical failure due to bodily movements. In the long term, these developments will advance smart wearables and precision medicine, democratizing at-home health monitoring. Furthermore, they will propel the flexible electronics sector, yielding more resilient foldable displays, soft robotics for disaster response, and advanced energy storage systems. Ultimately, this work will foster technological progress and elevate quality of life across society.

SUMMARY

Hydrogels, three-dimensional crosslinked polymer networks with high water content, have attracted significant attention in flexible electronics owing to their tissue-like mechanical properties, tunable electrical behavior, and excellent biocompatibility. However, achieving both low hysteresis and high toughness remains a significant challenge, as these properties are often mutually exclusive. This review summarizes design strategies to address this limitation by emphasizing the importance of maintaining network integrity and uniform stress distribution. Approaches such as optimizing network structures, modifying crosslinking mechanisms, incorporating nanostructures, and introducing higher-order architectures are discussed. The potential applications of these hydrogels in sensors, energy-harvesting devices, supercapacitors, and bioelectronics are highlighted, along with future challenges. This work aims to guide the development of high-performance hydrogels and advance their practical use in flexible electronic devices.

INTRODUCTION

Hydrogels are macromolecular materials comprising three-dimensional, crosslinked polymer networks with high water con-

tent.¹ These networks incorporate numerous hydrophilic groups, enabling versatile tuning of chemical composition, network architecture, mechanical properties, and biological functionality.^{2,3} The porous structure of hydrogels facilitates efficient water



molecule transport within polymer matrix. With an elastic modulus akin to natural tissues and excellent biocompatibility, hydrogels are extensively utilized in applications such as wearable devices, implantable sensors, artificial skin, drug delivery systems, and wound dressings.^{4–8} Recent advancements have led to the development of functional hydrogels that respond to environmental stimuli, including light, temperature, pH levels, electric fields, magnetic fields, and mechanical forces, keeping pace with the rapid evolution of smart materials.^{9–13}

Despite the significant potential of hydrogels for diverse applications, critical challenges must be addressed to enable their practical implementation. Hydrogels often experience complex, long-term deformation in applications, making mechanical properties critical.¹⁴ Conventional hydrogels typically exhibit limited mechanical strength or flexibility due to heterogeneous polymer density, irregular crosslinked networks, or inadequate energy dissipation, constraining their utility.¹⁵ Most hydrogels show a positive correlation between hysteresis and toughness. Low-toughness hydrogels have limited reversible energy dissipation during deformation, and their weak intrinsic bond strength compromises mechanical performance. Consequently, developing hydrogels with high toughness (defined by high tensile strength and strain) has become a research priority. Mechanical properties can be enhanced by tailoring chemical structures, optimizing microstructures, or introducing effective energy dissipation mechanisms.^{16,17} However, substantial energy loss (hysteresis phenomenon) is often observed during the stretching process of these high-toughness hydrogels under large deformation.¹⁸ Bond breakage induced by deformation reorganizes slowly, leading to unrecoverable energy dissipation. Over thousands of deformation cycles, accumulated energy loss can cause structural damage and failure.¹⁹ Minimizing energy dissipation is thus essential for optimizing hydrogel performance in practical applications.

The hysteresis of a hydrogel is defined as the fraction of energy dissipated during the recovery phase of deformation relative to the total energy required for deformation.²⁰ The calculation is expressed as follows²¹:

$$\Delta U_i = \int_{\text{Loading}} \sigma d\epsilon - \int_{\text{Unloading}} \sigma d\epsilon, \quad (\text{Equation 1})$$

$$H = \frac{\Delta U_i}{\int_{\text{Loading}} \sigma d\epsilon}, \quad (\text{Equation 2})$$

where ΔU_i represents the energy dissipation, calculated as the area enclosed by the loading-unloading. $\int_{\text{Loading}} \sigma d\epsilon$ is the area under the loading curve with the x axis, and $\int_{\text{Unloading}} \sigma d\epsilon$ is the area under the unloading curve with the x axis. H is the hysteresis.

The elasticity of a hydrogel represents the proportion of energy released during the deformation recovery process to the total energy required for the deformation itself, where low hysteresis corresponds to high elasticity.²² The toughness of a hydrogel refers to the total energy absorbed during the uniform deformation process until it breaks. The calculation formula is as follows²³:

$$T = \int_0^\epsilon \sigma d\epsilon, \quad (\text{Equation 3})$$

where T represents the toughness, defined as the integrated area below the stress-strain curves. ϵ is the tensile fracture strain, and σ is the tensile stress.

The energy dissipation of hydrogels during cyclic deformation mainly originates from molecular chain sliding and internal friction, chemical bond breakage, disruption of physical bonds, relaxation of dangling chains, and release of temporary entanglements.^{24,25} High toughness demands sufficient internal energy dissipation mechanisms within the hydrogel network to dissipate stress and inhibit elastic shrinkage.^{26,27} In contrast, low hysteresis requires minimal energy dissipation.^{28,29} That is, low mechanical hysteresis indicates a high reorganization rate of the polymer network, enabling rapid recovery to its initial state. Low electrical hysteresis, in turn, reflects high stability of ion or electron transport pathways, as well as rapid resistance recovery. Specifically, when the mechanical network recovers quickly, the ion or electron transport channels can also recover synchronously and rapidly, thus establishing a clear correlation between the two.³⁰ Low-hysteresis and high-toughness hydrogels are generally defined as those with a hysteresis of less than 10% and a toughness exceeding 1 MJ/m³.^{31,32} This inherent contradiction makes it challenging to simultaneously achieve low hysteresis and high toughness. Particularly, for hydrogel sensors, high toughness enables them to withstand large strains and thus achieve a broad sensing range.³³ Low hysteresis ensures that hydrogel sensors possess excellent fatigue resistance, long service life, and rapid responsiveness during repeated strain cycling for continuous monitoring.³⁴ In contrast, hydrogel sensors with high toughness and high hysteresis often suffer from poor signal stability due to irreversible energy dissipation, making them unsuitable for long-term monitoring. On the other hand, sensors made with low-toughness and low-hysteresis hydrogels tend to have a narrow sensing range and are mechanically fragile, prone to fracture under deformation. Xue et al. designed a strain sensor featuring low hysteresis, high sensitivity, and high linearity by employing a gradient stiffness sliding strategy.³⁵ Under rapid stretching conditions (2 mm·s⁻¹), the sensor maintained excellent performance stability for 2,000 cycles without noticeable signal drift or fluctuation. Therefore, balancing toughness and hysteresis in hydrogels remains a critical challenge.

The efficiency of storing and releasing energy is influenced by the level of elastic deformation (which represents energy storage) and the extent of energy dissipation (indicating energy loss).²⁰ Nature provides numerous examples exhibiting high toughness and superelasticity, such as the heart, muscles, joint cartilage, and spider silk. The remarkable elasticity of the heart allows it to withstand approximately 2.5 billion repetitive loading cycles throughout its lifespan.³⁶ Muscles can sustain millions of repeated stretching and contraction cycles due to their outstanding mechanical support properties.³⁷ Articular cartilage, which functions like a biological spring, absorbs mechanical loads between bones, experiences relatively high pressures, and elastically deforms to store and release energy during

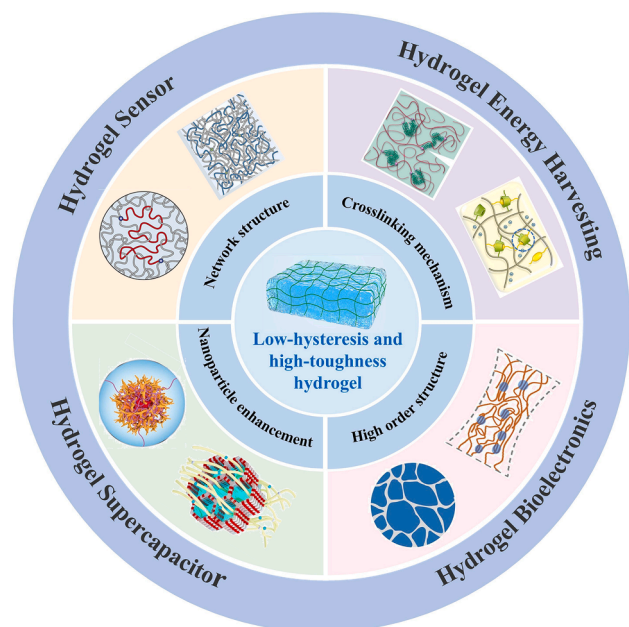


Figure 1. Recent strategies for designing low-hysteresis and high-toughness hydrogels and their potential applications

Strategies: Network structure (reproduced with permission,⁴⁵ copyright 2022, Wiley-VCH; reproduced with permission,²³ copyright 2024, Springer Nature), crosslinking mechanism (reproduced with permission,⁴⁶ copyright 2020, Springer Nature; reproduced with permission,⁴⁷ Copyright 2023, Springer Nature), nanomaterial reinforced (reproduced with permission,⁴⁸ copyright 2022, Wiley-VCH; reproduced with permission,⁴⁹ copyright 2023, Springer Nature), and higher-order structure (reproduced with permission,⁵⁰ Copyright 2024, Wiley-VCH; reproduced with permission,⁵¹ Copyright 2023, AAAS). Applications: sensors, energy-harvesting devices, supercapacitors, and bioelectrical systems.

movement.³⁸ Biological tissues have evolved specialized structures composed of elastin stabilized by various hydrogen bonds to efficiently dissipate energy.^{39,40} Spider silk, consisting of nanocrystalline regions composed of hydrogen-bonded polypeptide chains uniformly dispersed within an amorphous matrix, exhibits excellent superelasticity and high toughness.⁴¹ Inspired by these natural structures, Wang et al. designed a low-hysteresis composite material consisting of a matrix with low elastic modulus and fibers with a high elastic modulus, characterized by strong interfacial adhesion between the matrix and the fibers without sacrificing bonds.⁴² Similarly, Wibowo et al. incorporated conductive materials into an elastic matrix and leveraged the strong physical interactions between the matrix and the conductive phase to fabricate a composite film with high extensibility and low hysteresis.⁴³ The resulting sensor demonstrated exceptional electromechanical stability due to the elimination of stress relaxation mismatch between the elastic matrix and conductive filler during recovery.

Although these examples from nature have provided valuable theoretical guidance and inspiration for constructing hydrogels with low hysteresis and high toughness, the intrinsic relationships among various low-hysteresis mechanisms have not yet been systematically discussed. For example, hydrogels with en-

tangled double-network (DN) chains and those exhibiting strain-induced crystallization both effectively balance the contradiction between toughness and hysteresis, yet these hydrogels rely on distinct low-hysteresis mechanisms.^{23,44} It remains unclear whether there is a universal mechanism for preparing low-hysteresis hydrogels. Energy dissipation mechanisms that avoid the introduction of sacrificial bonds are essential for achieving low hysteresis but have not been comprehensively explored. Therefore, developing general and comprehensive principles to resolve the contradiction between low hysteresis and high toughness in hydrogels is imperative.

Here, this review aims to establish a theoretical foundation for creating hydrogels that exhibit both low hysteresis and high toughness. To the best of our knowledge, no systematic review focusing on design hydrogels that simultaneously achieve maximum toughness and minimal hysteresis has been reported previously. First, we review and classify recent strategies for preparing hydrogels exhibiting maximum toughness and minimal hysteresis and propose comprehensive design principles to resolve the inherent conflict between these two properties (Figure 1). Subsequently, we summarize the diverse applications of low-hysteresis and high-toughness hydrogels, including their uses in sensors, energy-harvesting devices, supercapacitors, and bioelectronics. Finally, the key challenges and potential future directions for research in this area are highlighted.

DESIGN STRATEGY OF LOW-HYSTERESIS AND HIGH-TOUGHNESS HYDROGELS

Many tough hydrogels improve their mechanical properties through the incorporation of energy dissipation mechanisms. Nevertheless, it is still difficult to attain both low hysteresis and high toughness at the same time, as conventional energy dissipation structures frequently struggle to recover quickly following deformation.⁵² A comprehensive understanding of low-hysteresis mechanisms, that is, minimizing energy dissipation, plays a crucial role in guiding the design of hydrogels that combine low hysteresis with high toughness. For the development of polymer gels that exhibit minimal hysteresis, it is crucial to enhance the storage of elastic energy while concurrently reducing or completely removing energy loss. A general principle to achieve this is maintaining structural homogeneity and ensuring uniform stress distribution within the polymer network during stretching. This section discusses representative cases from previous studies on hydrogels with low hysteresis and high toughness, categorizing them into four main strategies: optimizing network structures, modifying crosslinking mechanisms, enhancing nanostructures, and introducing higher-order architectures.

Network structure

The classical continuum theory used to predict hydrogel properties typically assumes a simplified model, wherein the three-dimensional polymer network is considered ideal and homogeneous.⁵³ However, numerous studies have demonstrated that actual hydrogel networks exhibit significant spatial heterogeneity,⁵⁴ characterized by regions of dense and loosely crosslinking domains coexisting within the same network.⁵⁵ Such microstructural inhomogeneity significantly influences the macroscopic

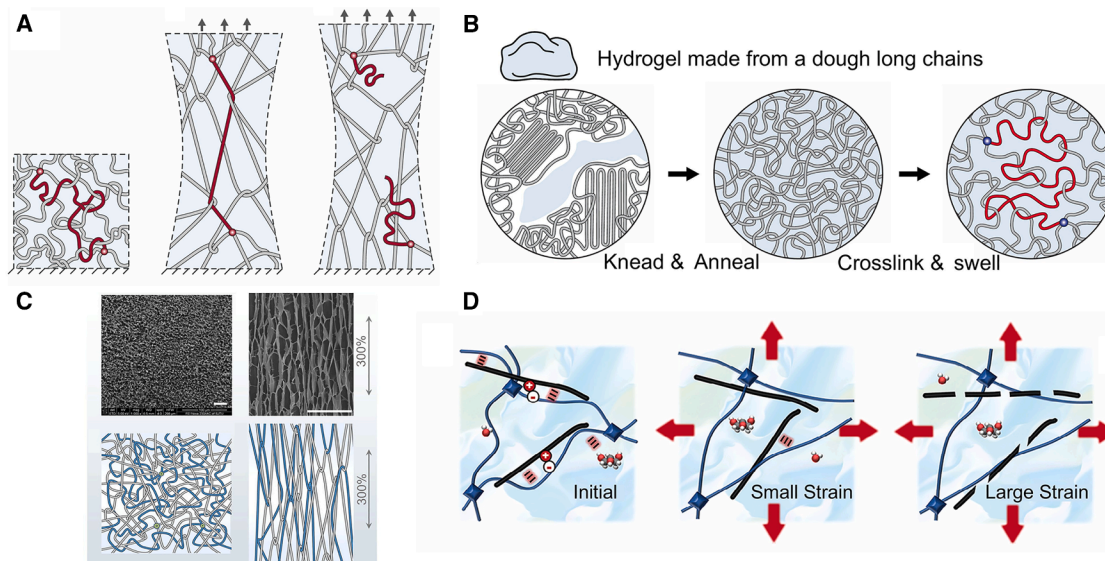


Figure 2. Strategies for preparing low-hysteresis and high-toughness hydrogels by optimizing the network structure

(A) Single-network chain entanglement. Reproduced with permission.⁵⁷ Copyright 2021, AAAS.

(B) Single-network chain entanglement dough hydrogel. Reproduced with permission.⁴⁵ Copyright 2022, Wiley-VCH.

(C) Double-network chain entanglement. Reproduced with permission.²³ Copyright 2024, Springer Nature.

(D) Interpenetrating polymer network. Reproduced with permission.⁵⁸ Copyright 2024, Wiley-VCH.

properties of hydrogels. Yang et al. reported that a heterogeneous network structure markedly affects hydrogel fracture behavior,⁵⁶ indicating that minimizing or eliminating this heterogeneity is crucial to addressing the challenges of achieving both low hysteresis and high toughness. Introducing physical entanglements or constructing interpenetrating polymer networks (IPNs) can enhance toughness while also preventing stress concentrations. Additionally, swelling hydrogels in suitable solvents can effectively reduce intermolecular friction, thereby minimizing the subsequent energy dissipation.

Single-network chain entanglement

Highly entangled hydrogels exhibit a significant degree of elasticity, akin to a spring, enabling them to efficiently transfer and store stress. When a highly entangled polymer is stretched, tension is transmitted along the chain and through entanglements, to numerous other chains. When a covalent bond in a chain is disrupted, the polymer disperses elastic energy throughout numerous extended long chains, which contributes to its high toughness. Additionally, the low interchain frictional resistance enables negligible hysteresis during cyclic loading.

Kim et al. designed a single-network polymer to address the conflict of tough hysteresis, characterized by long and highly entangled chains.⁵⁷ This dense entanglement facilitates the transfer of tension across multiple chains along the length of the polymer (Figure 2A). Upon immersion in water, the polymer attains an equilibrium state, resulting in a hydrogel that exhibits low hysteresis and high toughness. The hysteresis is negligible, remaining below 1% under cyclic tension across various strains. The near-perfect elasticity can be attributed to three key factors. First, the dense entanglement enables the hydrogel to preserve its intact network structure during stretching. Second, the flexibility of the entanglement allows the long polymer chains to slide consid-

erable distances before rupture occurs. Third, the low viscosity of water minimizes friction between the chains. Nian et al. developed a hydrogel composed of dough that exhibits both minimum hysteresis and significant toughness.⁴⁵ The dough consists of long polymer chains combined with a small quantity of water and a photoinitiator. This mixture is homogenized through kneading and annealing at elevated temperatures, resulting in tightly wound polymer chains (Figure 2B). Subsequently, the polymer chains are crosslinked under the action of ultraviolet light to form a network structure and then immersed in water to reach a balanced state. The resulting hydrogel demonstrates excellent elasticity, resistance to expansion, and toughness. First, the substantial water content in the expanded hydrogel diminishes friction among the chains. Second, the highly entangled structure of the hydrogel lacks sacrificial bonds. Due to the low viscosity of water, tangles within the expanded hydrogels can slip easily before rupture, rendering energy dissipation negligible. This ease of slippage is, in fact, the underlying reason for the concentration of tension along the long chains and the hydrogel's high toughness.

Double-network chain entanglement

The hysteresis of hydrogels can be reduced effectively by utilizing an elastic network that minimizes energy dissipation. Adjusting the network structure can enhance both the reversibility and elasticity of hydrogels.⁵⁹ Zhu et al. prepared DN hydrogels with a high degree of entanglement, which exhibited an energy dissipation-free structure. A significant number of physical entanglements function as efficient crosslinks within the first network.²³ The slip entanglement facilitates the creation of a highly uniform oriented structure in the hydrogel under tensile strain without energy dissipation (Figure 2C). The energy from external sources that is applied to the hydrogel does not get lost; instead, it is

preserved as entropy reduction within a highly oriented molecular chain, resulting in nearly 100% reversibility. Consequently, the high-entanglement DN structure successfully resolves the conflict between low hysteresis and high toughness in hydrogels.

Interpenetrating polymer network

The elastic IPN exhibits high flexibility and stretchability. Chen et al. designed a conductive organic hydrogel synthesized through the interpenetration of polyaniline (PANI) chains with a crosslinked poly(acrylamide-co-acrylic acid) network using a glycerin/water binary solvent.⁵⁸ The low interchain friction and the interpenetrating network structure contribute to its low hysteresis. Upon stretching, the network expands, while the PANI chain deforms (Figure 2D). This deformation leads to the destruction of non-covalent interactions, facilitating energy dissipation. The binary solvents serve as lubricants, reducing interchain friction within the network. Notably, the microstructure remains intact after cyclic loading, which can be attributed to the abundant porosity of the uniform network that promotes the dispersion of loading stress. The combination of the IPN structure and various non-covalent interactions endows organic hydrogels with maximum toughness and minimal hysteresis. Han et al. reported the preparation of a low-hysteresis semi-interpenetrating network hydrogel via *in situ* polymerization of acrylamide (AM) and ionic liquid.⁶⁰ In this hydrogel network, the poly(ionic liquid) serves as a physical crosslinked point, constructing a hydrogen-bond network that efficiently and rapidly dissipates energy, thus preventing stress concentration and hysteresis.⁶¹

Crosslinking mechanism

On the other hand, strong interactions between multifunctional crosslinkers and polymer chains can prevent the breakage of crosslinkers and chain slippage during repeated deformation cycles, thereby preserving the structural integrity of the polymer network and simultaneously achieving low hysteresis and high toughness.

Polyprotein crosslinking

Inspired by the natural load-bearing organizational structure, elastin that consists of tandem repeats of folded protein domains serves as a crosslinking agent for loosely stacked protein fibers. These fibers can unfold to dissipate mechanical loads and rapidly fold back to restore their original mechanical properties.^{62,63} Lei et al. proposed a network structure that includes an unstructured polymer as the permeating phase and a polyprotein as the crosslinking agent.⁴⁶ By embedding folded polyprotein crosslinkers, comprising eight tandem repeats of GB1, into a randomly wound polyacrylamide (PAM) network, they achieved a combination of low hysteresis and high toughness. The experiments demonstrate that the macroscopic deformation of the hydrogel primarily results from the extension of the permeable unstructured polymer rather than polyprotein crosslinker, as the crosslinker is mechanically bypassed (Figure 3A). Only when the unstructured chain is sufficiently tight does the force propagate to the polyprotein crosslink. Despite considerable elongation, the minimal extension of the polyprotein crosslinkers inhibits the unfolding of protein domains during stretching, enabling them to maintain their folded configuration under ultrahigh strain. Therefore, this design, which incorporates a

multi-protein crosslinker, challenges the conventional hysteresis-toughness correlation observed in traditional hydrogels.

Polypeptide crosslinking

Inspired by the ability of helical springs to absorb and store mechanical energy during deformation and release it during stress relief,⁶⁸ numerous studies have reported the incorporation of helical peptide chains into hydrogel networks to create hydrogels characterized by low hysteresis and high toughness.^{69,70} Liu et al. proposed a straightforward method for synthesizing hydrogels using peptide crosslinkers.⁶⁴ The integration of peptide chains structured as “molecular springs” not only mitigates the inhomogeneity of the network but also introduces a novel energy dissipation mechanism. Peptide-crosslinked hydrogels dissipate energy through the breaking of intramolecular hydrogen bonds within the spiral peptide chains. Similar to molecular-sized springs, these chains elongate into extended helical configurations under load, causing the intramolecular hydrogen bonds that maintain the helical structure to break. However, upon unloading, the peptide chains accurately refold back into their helical configuration, and the disrupted intramolecular hydrogen bonds nearly completely reorganize (Figure 3B). Consequently, the energy absorbed and stored by the system is released, resulting in a minimal hysteresis loop and enhanced elasticity. Introducing peptide crosslinking agents also imparted low hysteresis and high toughness to the eutectogel. Specifically, Zhang et al. introduced α -helical peptide segments into the deep eutectic solvent (DES) and produced continuously spun eutectogel fibers through a simple photopolymerization strategy.⁷¹ The α -helical peptide segments were employed to achieve energy dissipation, preparing fibers that mimic natural spider silk with high tensile strength (720 kPa) and exceptional elasticity (>95% recovery at 500% strain).

Dynamic micelles

Li et al. developed a solvent-induced dynamic micellar island structure method to copolymerize AM and acryloyl Pluronic 127 (PF127-DA) in aqueous solution, resulting in a novel multi-purpose hydrogel.⁶⁵ PF127-DA micelles serve as dynamic macroscopic crosslinkers; their deformation and the corresponding internal physical rearrangement function as a stress absorber under large deformation, providing an excellent energy dissipation mechanism (Figure 3C).⁷² By avoiding the introduction of sacrificial bonds to enhance toughness, the significant hysteresis typically associated with such bonds is eliminated.⁴² The hydrogel's remarkable stretchability, toughness, rapid resilience, and low hysteresis can be attributed to the flexibility and self-assembly capabilities of the PF127-DA molecular chain, which allows the PF127-DA micelles to break and reassemble quickly under external forces.⁷³

Sliding crosslinker

The ideal polymer network features uniformly distributed chains of equal length, minimal energy dissipation during deformation, and high resilience.⁷⁴ Xiong et al. developed a polymerizable rotaxane (PR) crosslinking agent by combining acrylated β -cyclodextrin (CD) with bile acids through precise host-guest recognition, followed by photopolymerization with AM to create a conductive hydrogel.⁴⁷ Due to the topological structure of PR, PR gels exhibit all the desirable characteristics, including low hysteresis. This is ascribed to the presence of polymerizable

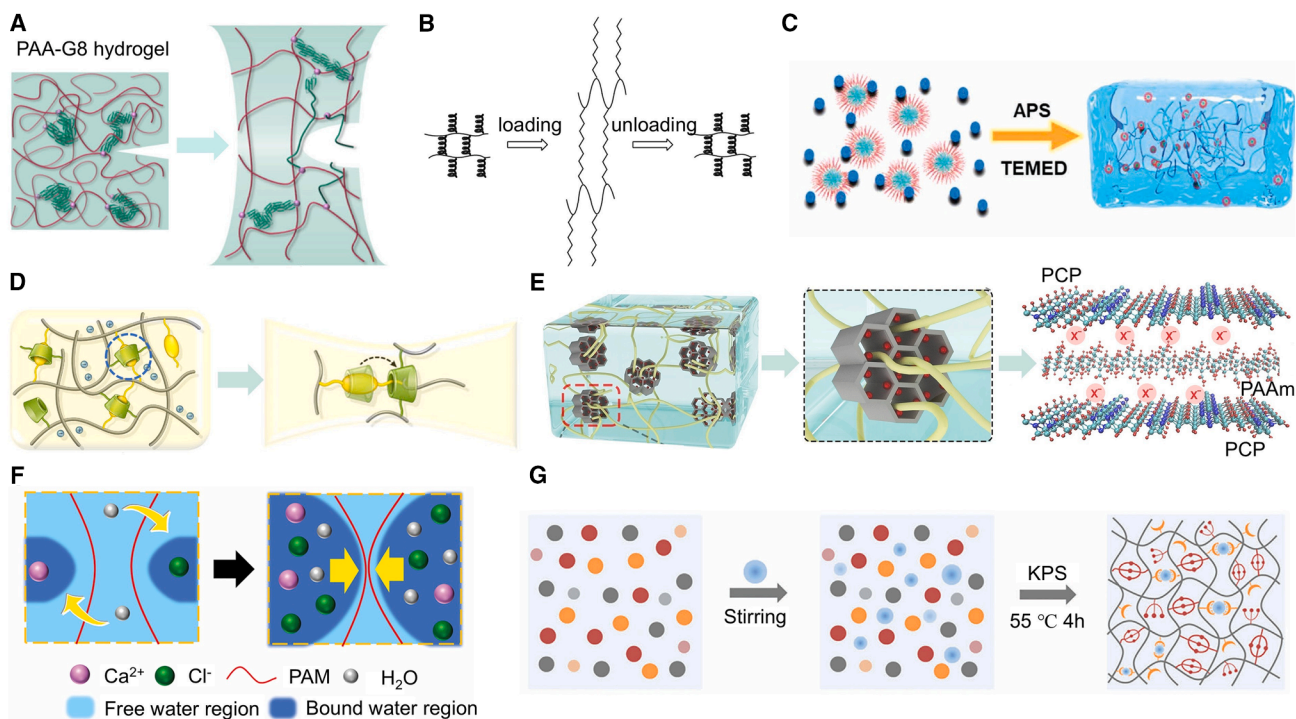


Figure 3. Strategies for preparing low-hysteresis and high-toughness hydrogels by modifying the crosslinking mechanism

(A) Polyprotein crosslinking. Reproduced with permission.⁴⁶ Copyright 2020, Springer Nature.

(B) Polypeptide crosslinking. Reproduced with permission.⁶⁴ Copyright 2021, Elsevier.

(C) Dynamic micelles. Reproduced with permission.⁶⁵ Copyright 2021, Wiley-VCH.

(D) Sliding crosslinker. Reproduced with permission.⁴⁷ Copyright 2023, Springer Nature.

(E) Cationic polymer. Reproduced with permission.⁶⁶ Copyright 2024, Wiley-VCH.

(F) Spatial constraint. Reproduced with permission.⁶⁷ Copyright 2023, Wiley-VCH.

(G) Supramolecular interaction crosslinking (hydrogen bond clusters). Reproduced with permission.³² Copyright 2024, Wiley-VCH.

crosslinkers, resulting in the creation of numerous mobile connections within the PR gels. The permanent and slippable nature of these movable junctions allows the PR gels to glide easily along the chain axis when external forces are applied, thereby alleviating stress concentrations on shorter chains and enabling the rearranged gel network to approximate the optimal polymer network.⁷⁵ Consequently, the dynamic mechanical interlocking and strong interactions among polymer segments in PR topological networks are crucial for the superior properties of these hydrogels (Figure 3D). The tensile properties of low-hysteresis slippable (SR) hydrogels are enhanced not through energy dissipation but rather by alleviating stress concentration resulting from sliding.

Cationic polymer

Xiong et al. developed a universal and simple approach for preparing hydrogels with low hysteresis by incorporating porous cationic polymers (PCPs) and adjustable anions that serve as dynamic physical crosslinkers. The topological configuration of the hydrogel is established through the interpenetration and winding of PCPs and polymer chain segments.⁶⁶ As a physical crosslinking agent, PCP provides numerous active sites that efficiently immobilize the polymer chain segments, preventing their slip and thus minimizing energy dissipation. This contributes to the high sensitivity of the hydrogel strain sensor (Figure 3E). Further-

more, based on the principle of adjustable ionic liquids, this approach can be extended to other PCP gels incorporating different metal halides.

Spatial constraint

Wang et al. proposed a novel method for designing hysteresis-free hydrogels, which is based on hydration-induced spatial constraints.⁶⁷ In this approach, spatial constraints replace the physical crosslinking of polymer chains, successfully avoiding stress concentration and hysteresis. The polymer chains can glide over one another to dissipate energy, leading to the creation of super-tough hydrogels characterized by minimal hysteresis (Figure 3F). Experiments and theories demonstrate that the differences in hydration between polymer chains and salt induce spatial limitations within the polymer chains by regulating the proportion of bound water to free water. This method represents a widely adopted strategy for synthesizing hysteresis-free hydrogels utilizing different salts and monomers.

Supramolecular interaction crosslinking

In stretchable ductile materials, hysteresis arises from the non-ideal fracture of the sacrificial bond under normal working conditions. Therefore, it is essential to ensure the stability of the sacrificial bond during normal operations, allowing it to dissipate energy effectively only when it is expected to break.⁷⁶ In recent years, supramolecular interactions, including non-covalent

interactions and dynamic covalent interactions, have been incorporated into chemically crosslinked hydrogels to address the trade-off between toughness and hysteresis. For example, the introduction of non-covalent interactions, such as B-N coordination,⁷⁷ metal coordination,⁷⁸ hydrophobic interaction,⁷⁹ and hydrogen bonding,⁸⁰ along with dynamic covalent interactions like the borate bond⁸¹ has effectively resolved this issue. The key to achieving minimal energy dissipation and low hysteresis lies in utilizing strong supramolecular interaction crosslinking, which reduces the separation of polymer chains and the degradation of sacrificial bonds.⁸² The rate at which supramolecular interactions recover also impacts the hysteresis of the hydrogel during stretching. A rapid recovery ensures that the internal network remains synchronized with external tensile deformation, thereby preserving elasticity while enhancing toughness and preventing breakage under normal operating conditions.⁸³

For instance, Wang et al. designed a one-pot heat-initiated polymerization of AM, N-tris(hydroxymethyl)methyl acrylamide, and ionic liquid, which were dissolved in core-shell structure-dispersed poly(3,4-ethylenedioxythiophene):poly(styrene sulfonate) (PEDOT:PSS) (Figure 3G). This process resulted in an all-polymer hydrogel exhibiting high toughness (1.22 MJ m^{-3}) and extremely low hysteresis (<5%).³² During the stretching cycle, the network of conductive hydrogels can be rapidly and efficiently restructured, resulting in extremely low hysteresis due to the non-covalent interactions dominated by abundant hydrogen bonds, which allow external forces to act on all polymer chains simultaneously. Similarly, Guo et al. constructed a dynamic hydrogen bond system by introducing a DES, composed of sulfobetaine methacrylate and glycerol, into AM and polyvinylpyrrolidone.⁸⁴ This DES regulates relaxation dynamics between hydrogen bonds and polymer chain segments. The resulting dense dynamic hydrogen bond network undergoes nearly simultaneous rupture and reorganization, enabling immediate bond energy recovery to equilibrium after loading/unloading cycles. This mechanism is key to achieving ultralow hysteresis (<3%) and high fracture strain (1,500%). This principle extends to other dynamic interactions. For example, Song et al. designed a hierarchical structure consisting of long-chain poly(acrylamide-co-1-vinyl-3-butylimidazolium bromide) and bacterial cellulose nanofibers, where the latter were dynamically covalently crosslinked via boronic acid.⁸⁵ Synergistic dynamic boronic ester bonding, hydrogen bonding, and electrostatic interactions enhanced mechanical properties, yielding a hydrogel with >1,000% elongation at break and hysteresis as low as 10.4%.

Nanomaterial reinforced

The heterostructures formed by incorporating nanomaterials into hydrogels are expected to resolve conflict between toughness and hysteresis across scales, from macroscopic to atomic.⁸⁶ Nanomaterials are frequently employed as mechanical reinforcement centers within hydrogels.^{87,88} Nevertheless, the limited active sites and the weak interaction between polymer chains and nanoparticles usually make it inevitable for the polymer chains in hydrogels to slip during repeated uniaxial tensile cycles.⁸⁹ However, after appropriate surface modification and functionalization, nanomaterials can significantly enhance their

interactions with polymer chains, effectively acting as stress transfer centers. This prevents chain slippage, maintains network integrity, and thereby achieves hydrogels with minimal hysteresis.

Silicon dioxide

Meng et al. described a method utilizing highly expanded, hyperbranched nanoparticles to enhance the mechanical properties of hydrogels.⁴⁸ In this hydrogel network, hyperbranched nanoparticles serve as the primary crosslinks, interconnected by polymer chains that are not temporarily entangled (Figure 4A). The unique topology and abundant surface hydroxyl groups of the hyperbranched nanoparticles increase the surface area, compensating for the reduction in polymer crosslinking density. Low crosslinking densities necessitate longer connecting chains, which tend to become heavily entangled; however, the high expansion of the hydrogels eliminates these temporary tangles, leaving only permanent ones that enhance elasticity. As anticipated, this hydrogel exhibits negligible energy dissipation during large deformations, resulting in no mechanical hysteresis. Similarly, Zhou et al. prepared a poly(acrylic acid-co-acrylamide) hydrogel crosslinked by silica nanoparticles through photodimerization and salting out hydrophilic ions.⁹⁰ The vinyl hybrid silica nanoparticle (VSNP) possesses a unique topology and rich surface hydroxyl groups, which facilitate a balance between strength and energy consumption. VSNP can spontaneously function as covalently crosslinked sites and stress transfer centers within the hydrogels. The ultrahigh surface-to-volume ratio of VSNP compensates for the diminished crosslinking density, thereby promoting robust physical interactions and effective stress transfer.⁹¹ As the polymer chains in the hydrogel are stretched, the VSNP acts as a stress transfer center, reinforcing the network. This effectively mitigates stress concentration within the hydrogel, preventing sample rupture prior to damage and resulting in low mechanical and electrical hysteresis.

Ji et al. designed biomimetic silica (BM-silica) nanoparticles, featuring circular polyamine chains embedded on their surface, to enhance PAM hydrogels.⁹² This unique surface structure of BM-silica facilitates robust interfacial interactions through the entanglement and localized topological folding of polymer chains. The transfer of load from the soft gel matrix to the rigid nanoparticles, along with the elastic gliding and unwinding of the molecular chains, effectively addresses the traditional conflict between hysteresis and toughness (Figure 4B). At the interface between PAM and BM-silica, there is an absence of sacrificial breaking of interface bonds, whether chemical or physical crosslinking, which leads to negligible energy dissipation and hysteresis.⁹⁵ In contrast, the interfacial interactions between PAM and BM-silica, coupled with the unrestricted movement of folded and entangled PAM chains within the hydrogel matrix, enable reversible deformation of PAM chains during elastic slipping and unwinding.⁹⁶ The nearly perfect elastic behavior exhibited by PAM/BM-silica differs significantly from that of previous interpenetrating DN hydrogels, which typically suffer from irreversible damage and substantial hysteresis, such as PAM/alginate hydrogels.⁹⁷

MXene

MXene nanosheets are prone to oxidation and present challenges in dispersion within aqueous solutions. Furthermore, the

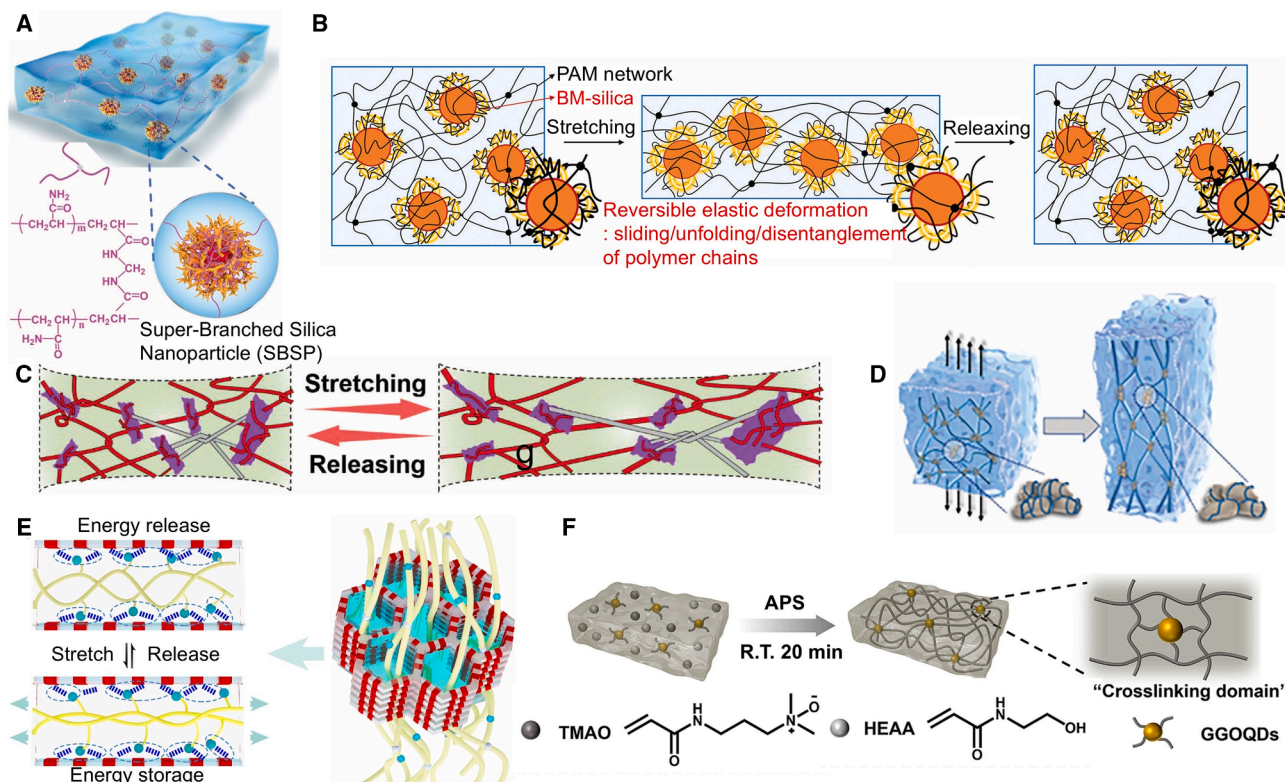


Figure 4. Strategies for preparing low-hysteresis and high-toughness hydrogels by enhancing nanostructures

- (A) Hyperbranched silicon. Reproduced with permission.⁴⁸ Copyright 2022, Wiley-VCH.
 (B) Biomimetic silicon. Reproduced with permission.⁹² Copyright 2023, Wiley-VCH.
 (C) MXene. Reproduced with permission.⁹³ Copyright 2024, Wiley-VCH.
 (D) $g\text{-C}_3\text{N}_4$. Reproduced with permission.⁸⁶ Copyright 2024, Wiley-VCH.
 (E) Covalent organic framework (COF). Reproduced with permission.⁴⁹ Copyright 2023, Springer Nature.
 (F) Graphene oxide. Reproduced with permission.⁹⁴ Copyright 2024, Elsevier.

weak interactions between MXene and the hydrogel network complicate the preparation of high-performance hydrogel sensors.⁹⁸

Liu et al. selected tannic acid (TA), which features a high density of hydroxyl groups, to encapsulate MXene nanosheets via hydrogen bonding. This approach significantly enhances the stability of MXene nanosheets in aqueous solutions.⁹⁹ Furthermore, the introduced TA generates numerous hydrogen bond interactions with the poly(hydroxyethyl acrylate) (PHEA) network. Specifically, the dense hydrogen bonding between the PHEA chains and TA@MXene provides an energy dissipation mechanism while restricting slip among the polymer chains. This interaction alleviates stress concentration, thereby improving energy dissipation efficiency and reducing mechanical hysteresis. Additionally, the rapid formation and breaking of hydrogen bonds during the stretching cycle preserve the high tensile strength and elastic recovery of the polymer network.

Zou et al. introduced a novel mechanism for the fabrication of highly entangled PAM/MXene hydrogels that do not require chemical crosslinkers.⁹³ In this approach, PAM molecular chains create numerous entanglements on the surface of MXene nanosheets, which preserves both the dynamic interactions and the

integrity of the network structure. Consequently, MXene nanosheets serve as effective stress transfer points, distributing stress across a broader range of polymer chains (Figure 4C). The novel strategy of “sliding entanglement island” significantly contributes to the hydrogels’ low mechanical hysteresis and high toughness.

$g\text{-C}_3\text{N}_4$

Liu et al. were the first to utilize $g\text{-C}_3\text{N}_4$ as the sole photoinitiator for the *in situ* polymerization of Zn^{2+} -crosslinked ternary polymers, resulting in the formation of chain entanglements within the heterostructured gel. This innovative approach produced a hydrogel characterized by low hysteresis and high elasticity.⁸⁶ The strategic integration of $g\text{-C}_3\text{N}_4$ with the terpolymer established a robust heterogeneous network, wherein each component is thoughtfully designed to exhibit complementary properties. The resultant hydrogel elastomer benefits from the synergistic effects of permanent entanglements arising from the interactions between $g\text{-C}_3\text{N}_4$ and the polymer chains, along with sparse ion crosslinking within the terpolymer matrix (Figure 4D). This collaboration effectively addresses the hysteresis-toughness trade-off in hydrogels at both macro- and micro-scales, endowing the hydrogel sensor with enhanced mechanical and sensing capabilities.

COF

Li et al. proposed a novel strategy for nanoconfined polymerization aimed at preparing tough, hysteresis-free hydrogels under large stretches.⁴⁹ Hydrogels are synthesized through crosslinking monomers within a covalent organic framework (COF) or molecular sieve nanochannel. The interpenetrating polymer segments effectively immobilize those that may slide under load (Figure 4E). The molecular potential energy of polymer fragments with reduced entropy, resulting from nanoscale constraints, increases when stretched, facilitating energy storage and thereby preventing energy dissipation and eliminating hysteresis. Specifically, rigid COF nanoparticles serve as centers for stress transfer and dissipation, mitigating stress concentration caused by segment breaks.¹⁰⁰ Additionally, the dense entanglement within the topological network enables the tension on one polymer chain to be efficiently transferred to adjacent chains, preserving the integrity of the network.^{14,101} This method presents a general strategy for synthesizing hydrogels, ionic gels, and organogels, effectively addressing the traditional conflict between large deformation and high elasticity.

Graphene oxide

Zhou et al. developed an innovative amphoteric hydrogel utilizing trimethylamine N-oxide derivatives and N-(2-hydroxyethyl) acrylamide as monomers, along with glycidyl methacrylate functionalized graphene oxide quantum dots (GGOQDs) serving as crosslinked agents.⁹⁴ The synthesized GGOQDs possess numerous physical and chemical crosslinking sites, which stabilize the network structures and minimize the slippage of the molecular chains (Figure 4F). This multistage crosslinked architecture allows GGOQDs to create a “crosslinked domain” within the hydrogel, thereby preserving the integrity of the hydrogel network during repeated stretches. The substantial tension is not only transferred to the neighboring molecular chains but also to the “crosslinked domain,” leading to a reduction in hysteresis and an enhancement in elasticity.

Higher-order structure

Tendons are made up of tough fibers that carry external loads and a flexible matrix that transports water. This heterogeneous structure provides tendons with exceptional load bearing under high mechanical stress, effectively reducing energy dissipation, and resulting in low hysteresis.¹⁰² Similarly, the remarkable mechanical strength, toughness, elasticity, and resilience of spider silk are attributed to its distinctive two-phase structure, where β -sheet nanocrystals composed of hydrogen-bonded polypeptide chains are uniformly embedded within an amorphous matrix, enabling it to endure millions of load cycles.¹⁰³ Such biological heterogeneity has inspired innovative composite material research. Introducing hierarchical structures into hydrogels can significantly improve their elasticity and ensure uniform stress distribution under loading conditions,¹⁰⁴ effectively mitigating hysteresis and resolving the contradiction between toughness and hysteresis.

Induced crystallization

Liu et al. designed a non-damaging strengthening approach for constructing SR hydrogels by utilizing strain-induced crystallization, wherein polyethylene glycol (PEG) chains are interconnected through slippable crosslinking composed of hydroxy-

propyl- α -CD rings.⁴⁴ In SR hydrogels, crosslinking allows for sliding along PEG chains, facilitating stress release within the network. Under uniaxial stretching, the crosslinked chains slide in proximity to one another, resulting in elongation of the polymer chains situated between the crosslinking points, which stretch uniformly in the direction of the applied force.¹⁰⁵ At significantly high strains, highly oriented PEG chains repeatedly form and break tightly packed structures through the processes of stretching and subsequent release (Figure 5A). The reversible formation and destruction of PEG crystals accounts for the nearly 100% rapid recovery elongation exhibited by SR hydrogels, surpassing that of covalently crosslinked PEG homogeneous hydrogels.

Similarly, Cao et al. described a strategy that utilizes scalable layered heterogeneous hydrogel fibers to produce soft bio-electronic sensors exhibiting high toughness (1.4 MJ m^{-3}) and low hysteresis (<7.6% at 200% strain) through a non-damaging toughening mechanism.⁵⁰ This mechanism involves dense long-chain entanglement and reversible strain-induced crystallization of sodium polyacrylate (PANa). Under continuous stretching, the highly wound PANa network undergoes deformation and rearrangement, accompanied by reversible strain-induced crystallization (Figure 5B), thereby enhancing the toughness of the hydrogel. Specifically, the original PANa hydrogel is an isotropic, highly entangled long-chain network that possesses structural stability and low crystallinity. As it stretches, the tension within the PANa chains is transmitted along their lengths and through entanglement to numerous other chains. With an increase in strain, the chains become oriented, forming crystalline domains that impede their sliding and fracturing, thereby improving the hydrogel's toughness. Upon release, the chains revert to a random configuration driven by entropy, resulting in high elasticity.

Microphase separation

Zhang et al. synthesized hydrogels characterized by high strength and low hysteresis through stationary phase separation.⁵¹ These hydrogels are formed by the interpenetration of hydrophilic and hydrophobic networks and can be categorized into water-rich and water-poor phases. The topological entanglement of these two networks effectively prevents phase separation (Figure 5C). At the microscopic scale, these two phases remain distinct. The water-rich phase is softer compared to the water-poor phase, resulting in the latter bearing the major load under hydrogel stretches. The significant difference in the modulus between the two phases facilitates the dispersion of stress from the water-rich phase to the water-poor phase. Consequently, the enhancement of the hydrogel arises from phase separation rather than merely the interpenetration of polymer networks. Both phases exhibit elasticity and maintain a strong adherence through topological entanglement, resulting in low hysteresis of the hydrogel. Overall, this hydrogel demonstrates superior properties compared to existing hydrogels, particularly in terms of low hysteresis and high strength.

Shen et al. constructed a unique microphase semi-separation network by combining PEDOT:PSS nanofibers with poly(vinyl alcohol) (PVA) to achieve high tensile strength and hysteresis-free performance in hydrogel strain sensors.¹⁰⁶ The PEDOT-rich semi-crystalline and PVA domains within the amorphous

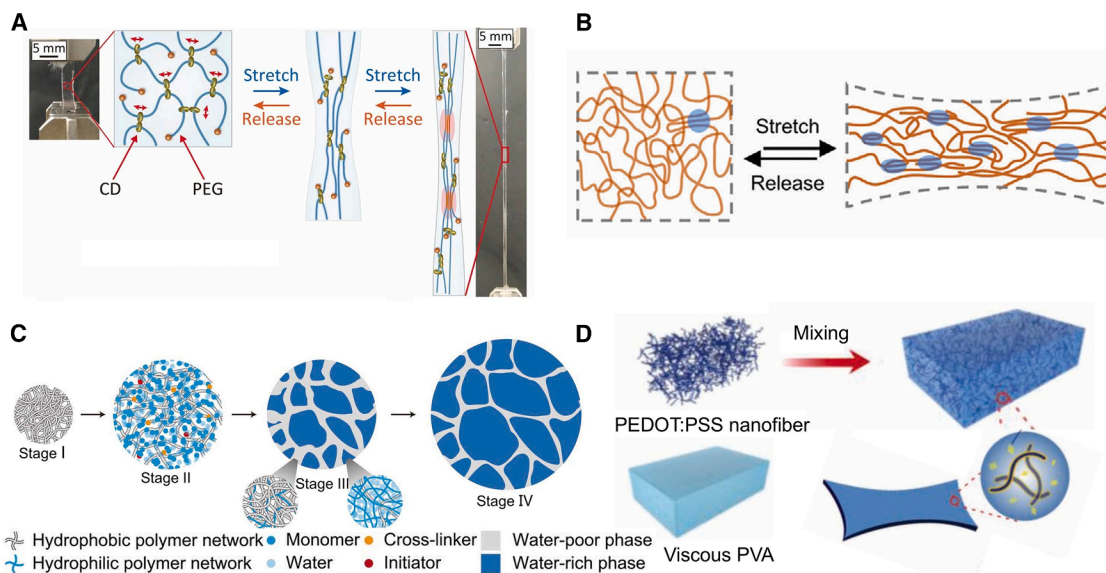


Figure 5. Strategies for preparing low-hysteresis and high-toughness hydrogels by introducing higher-order structure

(A) Strain-induced crystallization of slip-ring hydrogel. Reproduced with permission.⁴⁴ Copyright 2021, AAAS.

(B) Strain-induced crystallization of hydrogel fibers. Reproduced with permission.⁵⁰ Copyright 2024, Wiley-VCH.

(C) Phase separation. Reproduced with permission.⁵¹ Copyright 2023, AAAS.

(D) Microphase semi-separation. Reproduced with permission.¹⁰⁶ Copyright 2022, Wiley-VCH.

matrix are physically crosslinked using a continuous freeze-thaw technique, resulting in a phase configuration that interlocks to form a uniform and stable microphase semi-separated hydrogel network (Figure 5D). Multiple intermolecular interactions, including electrostatic interactions, hydrogen bonds, and chain entanglement, between the PEDOT, PSS, and polymer chains facilitate the merging and interlocking of the phase boundaries. By eliminating interface disengagement and sliding problems between conductive polymers and elastic hydrogels, this phase configuration significantly reduces hysteresis without compromising electrical and mechanical properties. Table 1 summarizes the relevant reports on the recent preparation of hydrogels with low hysteresis and high toughness using these methods.

Optimizing the network structure enables entropy elasticity-driven energy storage and release via highly entangled long-chain networks (Figure 6A). However, an ideal uniform network structure remains difficult to achieve, as it requires precise control over polymerization reaction conditions. Modifying the crosslinking mechanism involves incorporating crosslinking sites with rapid, reversible responsive properties to achieve efficient, recoverable energy dissipation (Figure 6B). Nevertheless, the design of such precise molecular crosslinking agents and their fabrication processes are complex, impeding large-scale application. Nanomaterial reinforcement leverages nanomaterials as multifunctional stress-transfer centers to achieve uniform stress distribution and suppress irreversible chain slippage (Figure 6C). However, the intrinsic dispersion challenges of nanomaterials, along with the need for precise regulation of interface interaction strength, have hindered the advancement of this strategy. Introducing higher-order structures mimics the heterogeneous architectures found in natural systems, enabling synergistic energy dissipation and elastic recovery through multi-

phase separation (Figure 6D). Yet, the difficulty in the controllable fabrication of complex structures and the inherent property anisotropy of such systems remain key limitations. Therefore, the future development of low-hysteresis and high-toughness hydrogels will require the integrated and coordinated application of these strategies.

The uniqueness of the four methods lies in the fundamental differences of the “source of energy reversibility,” which have resulted in differentiated energy dissipation mechanisms due to the different scales of action (Table 2). Optimizing the network structure focuses on “chain entanglement slip” at the chain scale. Modifying the crosslinking mechanism focuses on “dynamicity of crosslinking points” at the molecular scale. Nanomaterial reinforcement utilizes a “nanoscale interface-chain” effect to disperse stress at the mesoscopic scale. The introduction of higher-order structures enables hierarchical energy dissipation through multi-phase synergy at the macroscopic scale. In the future, cross-scale collaborative design of high-performance hydrogels will be necessary to achieve maximum toughness and minimum hysteresis, thereby meeting the performance requirements of flexible electronic devices.

APPLICATION OF LOW-HYSTERESIS AND HIGH-TOUGHNESS HYDROGELS IN FLEXIBLE ELECTRONICS

Flexible electronic devices based on hydrogels possess good stretchability and compressibility. Rationally engineered hydrogels can detect stimuli, including pressure, tension, and temperature, converting these inputs into electrical signals.^{107–109} Hydrogels with low hysteresis significantly enhance the long-term reliable stability of electronic devices.^{31,110} In this section, we discuss various applications of maximum-toughness and

Table 1. Recent representative design methods, materials, and mechanical properties of low-hysteresis and high-toughness hydrogels

Method	Hydrogel	Hysteresis (%)	Toughness (kJ/m ³)	Stretchability- ϵ (%)	Stress (kPa)	Modulus (kPa)	Fatigue threshold (J/m ²)	Reference
Network structure	PAM	≈ 0 ($\epsilon = 270$)	≈ 730	≈ 420	390	–	≈ 200	Kim et al. ⁵⁷
	PEG	≈ 0 ($\epsilon = 350$)	854	590	462	≈ 300	100	Nian et al. ⁴⁵
	HEDN	≈ 1 ($\epsilon = 200$)	2,490	≈ 350	3,000	–	–	Zhu et al. ²³
	P(AAm-co-AAc)/PANI	≈ 15 ($\epsilon = 100$)	216	482	≈ 110	–	–	Chen et al. ⁵⁸
	PAT ₂ V ₃	9 ($\epsilon = 500$)	400	900	108	16	–	Han et al. ⁶⁰
Crosslinking mechanism	PAA-G8	< 5 ($\epsilon = 1,000$)	≈ 700	$\approx 1,100$	110	12	≈ 126	Lei et al. ⁴⁶
	A ₆ PC23 _{1%}	< 9 ($\epsilon = 500$)	$> 2,500$	$> 1,250$	> 500	> 120	–	Liu et al. ⁶⁴
	PAM/PF127	≈ 10 ($\epsilon = 500$)	7,170	$\approx 1,200$	$\approx 1,200$	≈ 300	–	Li et al. ⁶⁵
	PR-gel	< 3 ($\epsilon = 300$)	270.7	830	78.1	–	–	Xiong et al. ⁴⁷
	PCP (Zn)-gel	7 ($\epsilon = 4,000$)	68,000	13,000	1,800	–	–	Xiong et al. ⁶⁶
	PAM-CaCl ₂	0.13 ($\epsilon = 1,000$)	9,440	$\approx 1,650$	$\approx 2,000$	20	–	Wang et al. ⁶⁷
	P(AM-THMA-ILs)/PP	5 ($\epsilon = 800$)	1,220	1,015	250	44	–	Wang et al. ³²
Nanomaterial reinforced	Hf-gel	≈ 1.3 ($\epsilon = 700$)	≈ 600	$\approx 1,200$	≈ 150	–	–	Meng et al. ⁴⁸
	PAM/BM-silica	≈ 0 ($\epsilon = 1,000$)	$\approx 1,100$	1,400	250	13.6	–	Ji et al. ⁹²
	PAM-MXene	< 7 ($\epsilon = 100$)	1,340	≈ 900	175	–	–	Zou et al. ⁹³
	PHEA-TA@MXene	≈ 5 ($\epsilon = 500$)	276.3	690	85	12.5	–	Liu et al. ⁹⁹
	TCPH10	7.25 ($\epsilon = 60$)	2,040.76	1,500	330	21.7	–	Liu et al. ⁸⁶
	NCP	10 ($\epsilon = 8,000$)	87,700	17,580	$\approx 1,000$	96	–	Li et al. ⁴⁹
	PTH-G	3.6 ($\epsilon = 150$)	46.8	≈ 320	≈ 25	15.4	–	Zhou et al. ⁹⁴
High-order structure	SR-gel	< 3 ($\epsilon = 800$)	22,000	$\approx 1,300$	$\approx 5,500$	–	–	Liu et al. ⁴⁴
	LHHFs	8 ($\epsilon = 200$)	1,400	≈ 500	≈ 280	–	–	Cao et al. ⁵⁰
	PEA-PAAc	16.6% ($\epsilon = 100$)	$\approx 7,400$	≈ 510	6,900	–	–	Zhang et al. ⁵¹

HEDN, highly entangled double network; P(AAm-co-AAc)/PANI, poly(acrylamide-co-acrylic acid)/polyaniline; PAA-G8, polyacrylamide-GB1; PR, polymerizable rotaxane; PCP, porous cationic polymer; P(AM-THMA-ILs)/PP, poly(acrylamide-*N*-[tris(hydroxymethyl)methyl]acrylamide-1-butyl-3-vinylimidazolium bromide)/PEDOT:PSS; Hf, hysteresis-free; NCP, nanoconfined polymerization; PTH-G, zwitterionic polymer hydrogel; SR, slide-ring; LHHFs, layered heterogeneous hydrogel fibers. Some of the work reported in the table has a toughness that did not reach 1 MJ/m³, but through its method design, compared to the original hydrogel, the hysteresis has been reduced while the toughness has increased by 5–10 times.

minimal-hysteresis hydrogels in flexible electronic, such as sensors, energy-harvesting devices, supercapacitors, and bioelectrical systems.

Hydrogel sensors

Hydrogel-based flexible sensors exhibit high sensitivity and rapid response, making them widely applicable in human-computer interaction, electronic skin, healthcare, aerospace, and environmental monitoring.^{111–115} The performance of these hydrogel sensors is significantly influenced by mechanical hysteresis during cyclic loading. Flexible hydrogel sensors characterized by substantial hysteresis often exhibit residual strain and baseline drift during signal cycle detection, which undermines their ability to accurately predict physical deformation and results in poor long-term signal stability.^{116,117} Conversely, low-hysteresis hydrogels can be effectively utilized as resistance strain sensors. When an external force is applied, the internal conductive network undergoes alterations, leading to a change in resistance. These low-hysteresis hydrogels possess remarkable mechanical robustness, enabling them to withstand cyclic and severe loads, and are well suited for long-term monitoring

of various physiological signals, including motion detection, sound vibrations, electrocardiograms, and electromyography.

For example, Xu et al. synthesized a low-hysteresis hydrogel-based strain sensor by combining hydroxypropyl methyl cellulose (HPMC), PEDOT:PSS, and chemically crosslinked PAM.¹¹⁸ This hydrogel demonstrates high tensile strength and excellent elasticity due to the abundant hydrogen bonds formed between the chains of HPMC, PEDOT:PSS, and PAM. The prepared strain sensor exhibits extremely high sensitivity and remarkable stability. It is suitable for human wearable devices to monitor both large movements, such as those of human fingers, wrists, and knee joints, and subtle activities, including facial expressions and voice recognition. Notably, it can also function as a bioelectrode for detecting electrophysiological signals related to heart activity and electromyographic signals from wrist flexors, performing comparably to commercial electrodes (Figure 7A). Beyond its application as a strain sensor, low-hysteresis hydrogels can be utilized in three-dimensional (3D) printing to create pressure sensors characterized by fine layered structures and high sensitivity. Li et al. developed an organic hydrogel with low hysteresis and significant toughness through extensive dynamic physical crosslinking and

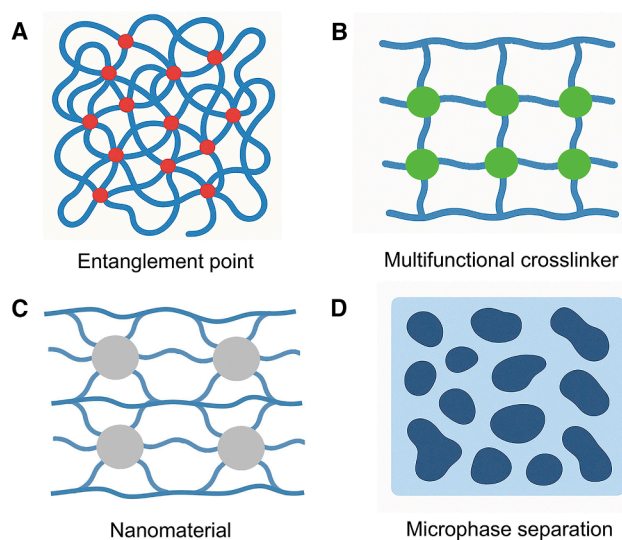


Figure 6. Mechanisms for designing low-hysteresis and high-toughness hydrogels

- (A) Optimizing network structures.
 (B) Modifying crosslinking mechanism.
 (C) Enhancing nanostructures.
 (D) Introducing higher-order architectures.

the formation of abundant hydrogen bonds among microgel, starch particles, glycerol, and acrylic acid.¹¹⁹ By employing 3D printing technology, they produced a cone-shaped sensor with ultrahigh-pressure sensitivity capable of recognizing human handwriting. The micro-structured sensor and the 3D printed anisotropic gel are integrated into a bionic multi-dimensional flexible sensor designed for the directional recognition of external forces and human movement (Figure 7B). Huang et al. further advanced the sensing applications of low-hysteresis hydrogels through the integration of machine learning techniques. They developed PAM/sodium hyaluronate (HA)/montmorillonite (MMT) hydrogels utilizing a dual physical crosslinking strategy.¹²⁰ PAM undergoes crosslinking via hydrophobic interactions, while HA enhances chain entanglement and MMT serves as a stress dissipation center and a physical crosslinking agent. The resulting synthetic hydrogels exhibit remarkably low hysteresis and near-perfect elasticity. Their highly elastic network can be engineered as a pressure sensor capable of distinguishing individual typing pat-

terns. After training with deep learning algorithms, users can be identified with a high degree of accuracy (Figure 7C). Consequently, these hydrogels are anticipated to be integrated into keyboards to enhance data privacy by accurately identifying users. Similarly, Entifar et al. designed a highly stretchable, low-hysteresis hydrogel film that is capable of precise motion sensing.¹²¹ When integrated with machine learning for action classification, it achieved 100% accuracy. Composed of carboxymethyl cellulose, PVA, and PEDOT:PSS, this hydrogel exhibits extremely low electrical hysteresis (0.101% at 50% strain) and excellent mechanical strength (0.525 MJ·m⁻³). These properties were achieved by optimizing the content of crosslinking agent PEG diglycidyl ether (PEGDE), which promotes covalent binding between polymer chains.

During temperature variations, the resistance change of a low-hysteresis hydrogel-based temperature sensor exhibits negligible hysteresis, thereby ensuring stable temperature sensing performance. Si et al. introduced a gel-assisted polymerization strategy to synthesize an innovative starch/PAM/borax/glycerol ionic hydrogel.⁸¹ The reversible network, formed by hydrogen bonds and coordination bonds, endows ionic hydrogel with remarkable elasticity, minimal internal friction, and effective energy dissipation capabilities. The ionization of Na₂B₄O₇ is particularly sensitive to fluctuations in temperature and humidity. This exceptional thermal sensitivity allows ionic hydrogels to be utilized for personal health monitoring. For instance, when volunteers' body temperatures increased from normal levels to fever states, the relative resistance rose by approximately 40%, a significant variation that can be employed to monitor a patient's temperature (Figure 7D).

Hydrogel energy-harvesting devices

In recent years, hydrogel-based triboelectric nanogenerators (TEGs) have been widely applied in electronic skin and wearable devices, as they can convert mechanical vibrations into electrical energy through triboelectric effects and electrostatic induction.^{126,127} TEGs are capable of continuously powering electronic devices by harvesting energy generated from everyday human movements.^{128,129} The exceptional toughness, superelasticity, high conductivity, and biocompatibility of hydrogels position them as ideal candidates for TENG applications.^{130,131} However, conventional hydrogels exhibit low frictional charge and a pronounced hysteresis effect during operation, which can result in diminished output power, material

Table 2. Comparison of different mechanisms for designing hydrogels with low hysteresis and high toughness

Strategies	Reversible bonds	Network structure	Energy dissipation pathways
Network structure	physical entanglement (entropy elasticity)	highly uniform physical entanglement	chain segment reversible sliding and orientation
Crosslinking mechanism	dynamic reversible bond	uniform dynamic crosslinking point	reversible fracture and recombination of dynamic bonds
Nanomaterial reinforced	interfacial reversible interaction	nanoparticles and polymer chains are uniformly interlocked	rearrangement of interface interactions and stress transfer
Higher-order structure	multicomponent synergistic change	heterogeneous structure with microphase separation	multiphase hierarchical dissipation

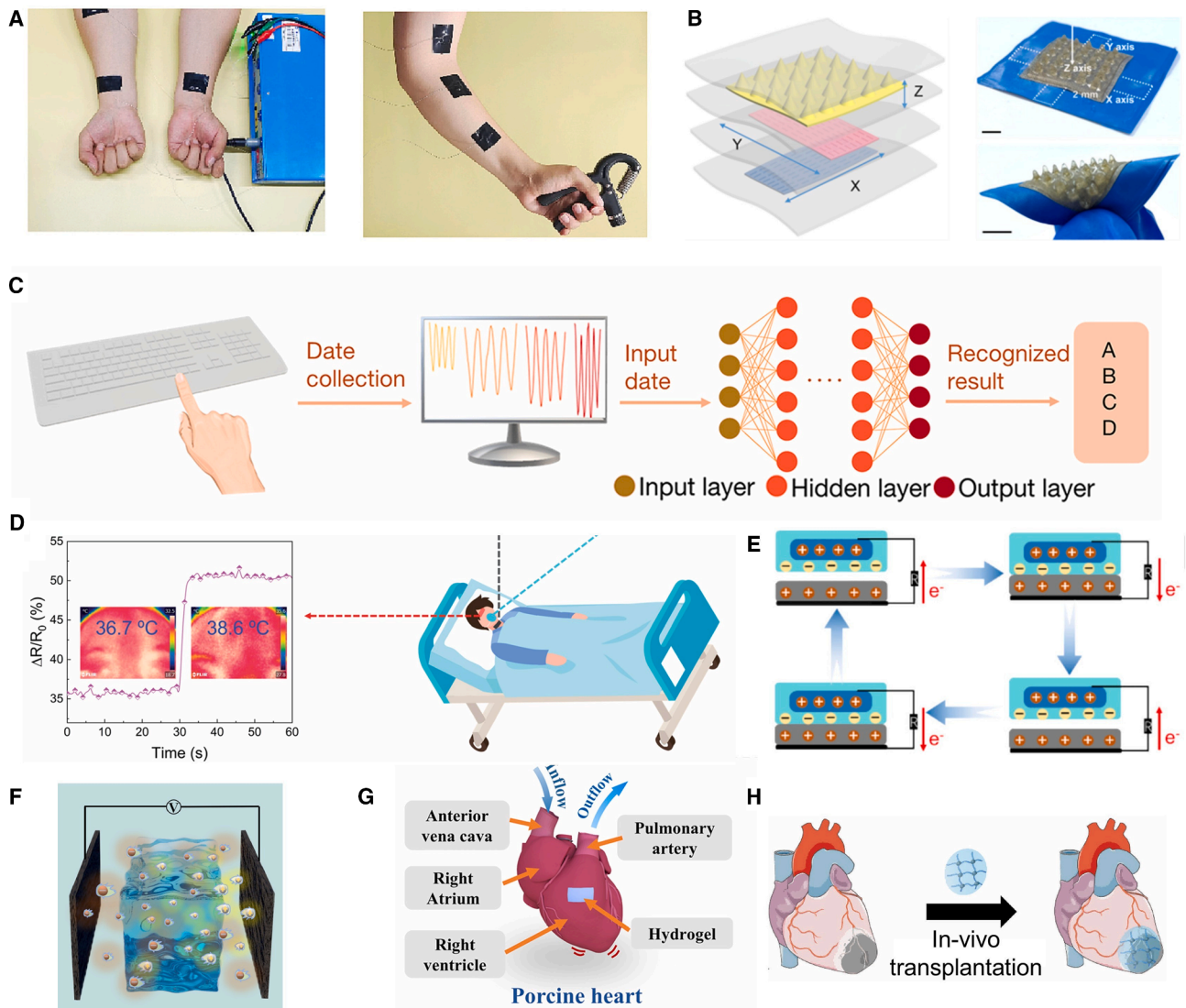


Figure 7. Application of low-hysteresis and high-toughness hydrogels

- (A) Bioelectrodes to detect electroencephalographic and electromyographic signals. Reproduced with permission.¹¹⁸ Copyright 2023, Elsevier.
 (B) 3D printed high-sensitivity pressure sensors. Reproduced with permission.¹¹⁹ Copyright 2024, Elsevier.
 (C) Hydrogel sensors for machine learning. Reproduced with permission.¹²⁰ Copyright 2024, ACS.
 (D) Temperature sensors to monitor the patient's temperature. Reproduced with permission.⁸¹ Copyright 2022, The Royal Society of Chemistry.
 (E) Hydrogel-based TENG. Reproduced with permission.¹²² Copyright 2025, Elsevier.
 (F) Hydrogel-based supercapacitors. Reproduced with permission.¹²³ Copyright 2024, Elsevier.
 (G) Implanted electrodes detect heart beats. Reproduced with permission.¹²⁴ Copyright 2022, The Royal Society of Chemistry.
 (H) Implantable bioelectronic patches. Reproduced with permission.¹²⁵ Copyright 2023, Wiley-VCH.

fatigue, and unstable electrical signals in TENGs. The development of low-hysteresis hydrogels enables them to maintain high elasticity and effectively harvest energy under prolonged mechanical stimulation.

Zou et al. designed an innovative structural organic hydrogel utilizing boric acid as a bridging agent, where the molecular chains of PAM and the solvent ethylene glycol (EG) are interconnected through B-N coordination bonds and borate ester bonds.⁸³ EG serves as an effective lubricant, minimizing internal friction among molecules. This dilatation effect aids in alleviating

temporary tangles within the hydrogel system. The resulting organic hydrogels exhibit exceptional tensile properties, minimal hysteresis, long-term stability, and low energy loss. The TENG, which incorporates the gel into a sandwich structure, can consistently convert mechanical motion into electricity, thereby powering small electronic devices and enabling energy harvesting (Figure 7E). Similarly, a hydrogel with reduced mechanical hysteresis, also designed by Zou et al., demonstrates significant potential for TENG applications.¹²² The nanoconfined mechanism provided by MXene within the hydrogel, along with the bridging

effect of chitosan, contributes to its low mechanical hysteresis and high conductivity. The bridging effect effectively elongates the polymer chain, enhancing stress transfer efficiency and diminishing mechanical hysteresis. Additionally, the nanoconfined further mitigates the occurrence of mechanical hysteresis by enveloping defects. The low-hysteresis hydrogel was integrated into a TENG as an energy-harvesting device, achieving an ultra-high-pressure sensitivity of 9.95 V kPa^{-1} .

Hydrogel supercapacitors

Supercapacitors are essential electronic components for enabling the wearability of flexible electronic systems.^{132,133} Typically, a supercapacitor comprises two external electrodes and an intermediate electrolyte.¹³⁴ Hydrogels serve as ideal electrolytes for flexible supercapacitors due to their liquid-like conductivity, solid-state stability, and excellent flexibility.^{135–138} During repeated charging and discharging cycles, supercapacitors impose cyclic loads on the hydrogel electrolyte, which may result in the formation of cracks and hysteresis, ultimately leading to the failure of the hydrogel supercapacitor. However, supercapacitors utilizing low-hysteresis hydrogels can rapidly and completely recover during stretching, thereby minimizing fatigue effects. This significantly enhances the reliability and durability of the devices, enabling them to maintain stable energy output under prolonged dynamic deformation conditions.

Zhao et al. developed a novel DN hydrogel electrolyte characterized by excellent tensile properties and minimal hysteresis.¹²³ This DN structure is achieved through hydrogen bonding and dipole interactions. The incorporation of lithium bis(trifluoromethane sulfonyl)imide facilitates interactions between fluorine atoms and the polymer network via hydrogen bonds, dipoles, and electrostatic forces. This interaction densifies the network structure, significantly enhancing its fatigue resistance and reducing the hysteresis effect of the hydrogel. The assembled supercapacitor demonstrates stable energy output, even under bending or compressive deformation, without fluctuations in signal (Figure 7F).

Hydrogel bioelectronics

To ensure the reliability of bioelectronic devices, it is crucial to maintain stable and strong adhesion between these devices and biological tissues.^{139,140} Traditionally, bioelectronic devices have relied on methods such as surgical sutures or physical connections. However, hydrogel-based implantable bioelectronic materials, known for their excellent biocompatibility and adjustable adhesion, as well as their mechanical and electrical properties, effectively address the mechanical mismatch at the biological tissue interface and significantly reduce immune rejection.^{141–144} Conventional hydrogels often exhibit considerable hysteresis and rupture during prolonged cyclic deformation, which can compromise long-term stability and sustainability. In contrast, the low-hysteresis properties of hydrogel-based implanted bioelectronics enable them to endure long-term stress, showcasing great potential in tissue engineering, nerve signal recording, implantable electrodes, and various biomedical applications.

Liu et al. proposed a multi-scale design principle for the preparation of self-reinforcing composite hydrogels with ionic conductivity, consisting of one phase as a conventional PAM gel

and another phase as a highly entangled PAM gel.¹²⁴ The composite hydrogel exhibited extremely low hysteresis (<3%) and excellent tensile strain (320%). The assembled strain sensor demonstrated excellent biocompatibility and was attached to a pig heart to capture the heartbeat signal (Figure 7G). The resistance varied 500 times in accordance with the heartbeat, and the signal remained stable. Shen et al. reported a new synthesis strategy for crosslinking PAM hydrogels using curcumin nanoparticles with a core-shell structure.¹²⁵ The nano-enhanced hydrogel exhibits excellent elasticity and no hysteresis phenomenon, enabling its use in synchronous monitoring of cardiac electrophysiological signals and repairing infarcted myocardial tissue. The extremely low hysteresis property ensures highly stable resistance signals, facilitating reliable real-time monitoring of myocardial healing throughout the myocardial infarction repair process (Figure 7H).

Conclusion and prospects

The rapid advancement of hydrogels has facilitated their widespread application across numerous fields. However, the inherent contradiction between achieving low hysteresis and high toughness remains a significant limitation for practical applications. Recently, substantial development has been made in addressing this issue through innovative structural and compositional designs. This review focuses on fundamental principles and mechanisms underlying the fabrication of hydrogels exhibiting both low hysteresis and high toughness, covering strategies such as network structure modulation, modification of crosslinking mechanisms, incorporation of nanostructures, and introduction of higher-order architectures. General strategies ensuring network integrity and uniform stress dispersion during deformation are also highlighted. Although hydrogels with optimized toughness and low hysteresis have already shown potential applications in sensors, energy-harvesting devices, supercapacitors, and bioelectronics, significant challenges remain. First, establishing robust theoretical models is crucial to elucidate molecular-level relationships between hydrogel toughness, hysteresis, and other mechanical properties (e.g., modulus and fatigue resistance). Utilizing artificial intelligence methodologies may further enhance overall hydrogel performance. Second, achieving multi-functional compatibility within flexible electronic applications requires integrating advanced properties, such as self-healing, power generation, biocompatibility, strong adhesion, and shape memory. Finally, addressing environmental stability, including resistance to extreme temperature, dehydration, and underwater osmotic pressure, remains critical. Recent developments in low-hysteresis ionic gels have partially addressed these challenges.^{145–148} Overcoming these challenges promises revolutionary advancements and broader practical applications for hydrogels exhibiting combined high toughness and minimal hysteresis in the future.

ACKNOWLEDGMENTS

The authors thank the support of the National Key R&D Program of China (2024YFB3816000 and 2024FYB3814102), National Natural Science Foundation of China (nos. 52401258, 52125205, 52250398, and 52192614), Natural Science Foundation of Beijing Municipality (L223006 and 2222088), Shenzhen Science and Technology Program (grant no. KQTD20170810105439418), and Fundamental Research Funds for the Central Universities.

DECLARATION OF INTERESTS

The authors declare no competing interests.

REFERENCES

- Li, X., and Gong, J.P. (2024). Design principles for strong and tough hydrogels. *Nat. Rev. Mater.* 9, 380–398. <https://doi.org/10.1038/s41578-024-00672-3>.
- Zhao, X. (2014). Multi-scale multi-mechanism design of tough hydrogels: building dissipation into stretchy networks. *Soft Matter* 10, 672–687. <https://doi.org/10.1039/C3SM52272E>.
- Yuan, Y., Zhang, Q., Lin, S., and Li, J. (2025). Water: The soul of hydrogels. *Prog. Mater. Sci.* 148, 101378. <https://doi.org/10.1016/j.pmatsci.2024.101378>.
- Li, Z., Lu, J., Ji, T., Xue, Y., Zhao, L., Zhao, K., Jia, B., Wang, B., Wang, J., Zhang, S., and Jiang, Z. (2024). Self-Healing Hydrogel Bioelectronics. *Adv. Mater.* 36, 2306350. <https://doi.org/10.1002/adma.202306350>.
- Hu, L., Chee, P.L., Sugiarto, S., Yu, Y., Shi, C., Yan, R., Yao, Z., Shi, X., Zhi, J., Kai, D., et al. (2023). Hydrogel-Based Flexible Electronics. *Adv. Mater.* 35, 2205326. <https://doi.org/10.1002/adma.202205326>.
- Li, X., Lin, Y., Cui, L., Li, C., Yang, Z., Zhao, S., Hao, T., Wang, G., Heo, J.-Y., Yu, J.-C., et al. (2023). Stretchable and Lithography-Compatible Interconnects Enabled by Self-Assembled Nanofilms with Interlocking Interfaces. *ACS Appl. Mater. Interfaces* 15, 56233–56241. <https://doi.org/10.1021/acsami.3c11760>.
- Qin, T., Li, K., Liu, Y., Xu, Z., and Gao, C. (2023). Low-Concentration Hydrogel Polyelectrolyte with In Situ Formed Interphases Enables 2.7 V Aqueous Pouch Cell. *Adv. Energy Mater.* 13, 2300733. <https://doi.org/10.1002/aenm.202300733>.
- Bao, R., Tao, J., Zhao, J., Dong, M., Li, J., and Pan, C. (2023). Integrated intelligent tactile system for a humanoid robot. *Sci. Bull.* 68, 1027–1037. <https://doi.org/10.1016/j.scib.2023.04.019>.
- Zhu, T., Ni, Y., Biesold, G.M., Cheng, Y., Ge, M., Li, H., Huang, J., Lin, Z., and Lai, Y. (2023). Recent advances in conductive hydrogels: classifications, properties, and applications. *Chem. Soc. Rev.* 52, 473–509. <https://doi.org/10.1039/D2CS00173J>.
- El Sayed, M.M. (2023). Production of Polymer Hydrogel Composites and Their Applications. *J. Polym. Environ.* 31, 2855–2879. <https://doi.org/10.1007/s10924-023-02796-z>.
- Niu, H., Yin, F., Kim, E.-S., Wang, W., Yoon, D.-Y., Wang, C., Liang, J., Li, Y., and Kim, N.-Y. (2023). Advances in flexible sensors for intelligent perception system enhanced by artificial intelligence. *InfoMat* 5, e12412. <https://doi.org/10.1002/inf2.12412>.
- Chen, J., Liu, F., Abdiryim, T., and Liu, X. (2024). An overview of conductive composite hydrogels for flexible electronic devices. *Adv. Compos. Hybrid Mater.* 7, 35. <https://doi.org/10.1007/s42114-024-00841-6>.
- Tian, L., Han, L., Wang, F., Shen, H., Li, Q., Zhu, L., and Chen, S. (2024). Dynamic Water Microskin Induced by Photothermally Responsive Interpenetrating Hydrogel Networks for High-Performance Light-Tracking Water Evaporation. *Adv. Energy Mater.* 15, 2404117. <https://doi.org/10.1002/aenm.202404117>.
- Li, W., Li, L., Zheng, S., Liu, Z., Zou, X., Sun, Z., Guo, J., and Yan, F. (2022). Recyclable, Healable, and Tough Ionogels Insensitive to Crack Propagation. *Adv. Mater.* 34, 2203049. <https://doi.org/10.1002/adma.202203049>.
- Sun, J.-Y., Zhao, X., Illeperuma, W.R.K., Chaudhuri, O., Oh, K.H., Mooney, D.J., Vlassak, J.J., and Suo, Z. (2012). Highly stretchable and tough hydrogels. *Nature* 489, 133–136. <https://doi.org/10.1038/nature11409>.
- Wang, X.-Q., Xie, A.-Q., Cao, P., Yang, J., Ong, W.L., Zhang, K.-Q., and Ho, G.W. (2024). Structuring and Shaping of Mechanically Robust and Functional Hydrogels toward Wearable and Implantable Applications. *Adv. Mater.* 36, 2309952. <https://doi.org/10.1002/adma.202309952>.
- Sakai, T., Matsunaga, T., Yamamoto, Y., Ito, C., Yoshida, R., Suzuki, S., Sasaki, N., Shibayama, M., and Chung, U.-i. (2008). Design and Fabrication of a High-Strength Hydrogel with Ideally Homogeneous Network Structure from Tetrahedron-like Macromonomers. *Macromolecules* 41, 5379–5384. <https://doi.org/10.1021/ma800476x>.
- Lu, X., Si, Y., Zhang, S., Yu, J., and Ding, B. (2021). In Situ Synthesis of Mechanically Robust, Transparent Nanofiber-Reinforced Hydrogels for Highly Sensitive Multiple Sensing. *Adv. Funct. Mater.* 31, 2103117. <https://doi.org/10.1002/adfm.202103117>.
- Han, Z., Lu, Y., and Qu, S. (2024). Design of Fatigue-Resistant Hydrogels. *Adv. Funct. Mater.* 34, 2313498. <https://doi.org/10.1002/adfm.202313498>.
- James, H.M., and Guth, E. (1943). Theory of the Elastic Properties of Rubber. *J. Chem. Phys.* 11, 455–481. <https://doi.org/10.1063/1.1723785>.
- Huang, B., Lv, Z., Zhang, M., Liu, J., Liu, H., Li, T., Fu, L., Lin, B., and Xu, C. (2025). Low mechanical-hysteresis soft materials: materials, design, and applications. *J. Mater. Chem. A* 13, 15427–15452. <https://doi.org/10.1039/D5TA01343G>.
- Lin, S., Zhou, Y., and Zhao, X. (2014). Designing extremely resilient and tough hydrogels via delayed dissipation. *Extreme Mech. Lett.* 1, 70–75. <https://doi.org/10.1016/j.eml.2014.11.002>.
- Zhu, R., Zhu, D., Zheng, Z., and Wang, X. (2024). Tough double network hydrogels with rapid self-reinforcement and low hysteresis based on highly entangled networks. *Nat. Commun.* 15, 1344. <https://doi.org/10.1038/s41467-024-45485-8>.
- Guo, H., Han, Y., Zhao, W., Yang, J., and Zhang, L. (2020). Universally autonomous self-healing elastomer with high stretchability. *Nat. Commun.* 11, 2037. <https://doi.org/10.1038/s41467-020-15949-8>.
- Li, C.-H., Wang, C., Keplinger, C., Zuo, J.-L., Jin, L., Sun, Y., Zheng, P., Cao, Y., Lissel, F., Linder, C., et al. (2016). A highly stretchable autonomous self-healing elastomer. *Nat. Chem.* 8, 618–624. <https://doi.org/10.1038/nchem.2492>.
- Luo, F., Sun, T.L., Nakajima, T., Kurokawa, T., Zhao, Y., Sato, K., Ihsan, A.B., Li, X., Guo, H., and Gong, J.P. (2015). Oppositely Charged Polyelectrolytes Form Tough, Self-Healing, and Rebuildable Hydrogels. *Adv. Mater.* 27, 2722–2727. <https://doi.org/10.1002/adma.201500140>.
- Sun, W., Xue, B., Fan, Q., Tao, R., Wang, C., Wang, X., Li, Y., Qin, M., Wang, W., Chen, B., and Cao, Y. (2020). Molecular engineering of metal coordination interactions for strong, tough, and fast-recovery hydrogels. *Sci. Adv.* 6, eaaz9531. <https://doi.org/10.1126/sciadv.aaz9531>.
- Han, S., Tan, H., Wei, J., Yuan, H., Li, S., Yang, P., Mi, H., Liu, C., and Shen, C. (2023). Surface Modification of Super Arborized Silica for Flexible and Wearable Ultrafast-Response Strain Sensors with Low Hysteresis. *Adv. Sci.* 10, 2301713. <https://doi.org/10.1002/advs.202301713>.
- Kamata, H., Akagi, Y., Kayasuga-Kariya, Y., Chung, U.-i., and Sakai, T. (2014). “Nonswellable” Hydrogel Without Mechanical Hysteresis. *Science* 343, 873–875. <https://doi.org/10.1126/science.1247811>.
- Yu, X., Wang, Y., Zhang, H., Li, Z., Zheng, Y., Fan, X., Lv, Y., Zhang, X., and Liu, T. (2023). Strain-Stiffening, Self-Healing, and Low-Hysteresis Physically Dual-Cross-Linked Hydrogels Derived from Two Mechanically Distinct Hydrogen Bonds. *Chem. Mater.* 35, 9287–9298. <https://doi.org/10.1021/acs.chemmater.3c02075>.
- Liu, F.-X., Jing, X., Yang, J., Mi, H.-Y., Feng, F.-Y., and Liu, Y.-J. (2025). Recent progress in low hysteresis gels: Strategies, applications, and challenges. *Nano Today* 67, 102601. <https://doi.org/10.1016/j.nantod.2024.102601>.
- Wang, W., Guo, P., Liu, X., Chen, M., Li, J., Hu, Z., Li, G., Chang, Q., Shi, K., Wang, X., and Lei, K. (2024). Fully Polymeric Conductive Hydrogels with Low Hysteresis and High Toughness as Multi-Responsive and

- Self-Powered Wearable Sensors. *Adv. Funct. Mater.* **34**, 2316346. <https://doi.org/10.1002/adfm.202316346>.
33. Bao, B., Zeng, Q., Li, K., Wen, J., Zhang, Y., Zheng, Y., Zhou, R., Shi, C., Chen, T., Xiao, C., et al. (2023). Rapid fabrication of physically robust hydrogels. *Nat. Mater.* **22**, 1253–1260. <https://doi.org/10.1038/s41563-023-01648-4>.
34. Yuan, H., Han, S., Wei, J., Li, S., Yang, P., Mi, H.-Y., Liu, C., and Shen, C. (2024). Noncovalent cross-linked engineering hydrogel with low hysteresis and high sensitivity for flexible self-powered electronics. *J. Energy Chem.* **94**, 136–147. <https://doi.org/10.1016/j.jechem.2024.02.039>.
35. Xue, F., Peng, Q., Ding, R., Li, P., Zhao, X., Zheng, H., Xu, L., Tang, Z., Zhang, X., and He, X. (2024). Ultra-sensitive, highly linear, and hysteresis-free strain sensors enabled by gradient stiffness sliding strategy. *npj Flex. Electron.* **8**, 14. <https://doi.org/10.1038/s41528-024-00301-7>.
36. Gumpangseth, T., Lekawanvijit, S., and Mahakkanukrauh, P. (2020). Histological assessment of the human heart valves and its relationship with age. *Anat. Cell Biol.* **53**, 261–271. <https://doi.org/10.5115/acb.20.093>.
37. Lin, S., Liu, J., Liu, X., and Zhao, X. (2019). Muscle-like fatigue-resistant hydrogels by mechanical training. *Proc. Natl. Acad. Sci.* **116**, 10244–10249. <https://doi.org/10.1073/pnas.1903019116>.
38. Kim, I.L., Mauck, R.L., and Burdick, J.A. (2011). Hydrogel design for cartilage tissue engineering: A case study with hyaluronic acid. *Biomaterials* **32**, 8771–8782. <https://doi.org/10.1016/j.biomaterials.2011.08.073>.
39. Li, H., Linke, W.A., Oberhauser, A.F., Carrion-Vazquez, M., Kerkvliet, J. G., Lu, H., Marszalek, P.E., and Fernandez, J.M. (2002). Reverse engineering of the giant muscle protein titin. *Nature* **418**, 998–1002. <https://doi.org/10.1038/nature00938>.
40. Fang, J., Mehlich, A., Koga, N., Huang, J., Koga, R., Gao, X., Hu, C., Jin, C., Rief, M., Kast, J., et al. (2013). Forced protein unfolding leads to highly elastic and tough protein hydrogels. *Nat. Commun.* **4**, 2974. <https://doi.org/10.1038/ncomms3974>.
41. Lee, S.-M., Pippel, E., Gösele, U., Dresbach, C., Qin, Y., Chandran, C.V., Bräuniger, T., Hause, G., and Knez, M. (2009). Greatly Increased Toughness of Infiltrated Spider Silk. *Science* **324**, 488–492. <https://doi.org/10.1126/science.1168162>.
42. Wang, Z., Xiang, C., Yao, X., Le Floch, P., Mendez, J., and Suo, Z. (2019). Stretchable materials of high toughness and low hysteresis. *Proc. Natl. Acad. Sci.* **116**, 5967–5972. <https://doi.org/10.1073/pnas.1821420116>.
43. Wibowo, A.F., Nagappan, S., Nurmaulia Entifar, S.A., Kim, J.H., Sembiring, Y.S.b., Han, J.W., Oh, J., Xie, G., Lee, G., Kim, J., et al. (2024). Recyclable, ultralow-hysteresis, multifunctional wearable sensors based on water-permeable, stretchable, and conductive cellulose/PEDOT:PSS hybrid films. *J. Mater. Chem. A* **12**, 19403–19413. <https://doi.org/10.1039/D4TA02875A>.
44. Liu, C., Morimoto, N., Jiang, L., Kawahara, S., Noritomi, T., Yokoyama, H., Mayumi, K., and Ito, K. (2021). Tough hydrogels with rapid self-reinforcement. *Science* **372**, 1078–1081. <https://doi.org/10.1126/science.aaz6694>.
45. Nian, G., Kim, J., Bao, X., and Suo, Z. (2022). Making Highly Elastic and Tough Hydrogels from Doughs. *Adv. Mater.* **34**, 2206577. <https://doi.org/10.1002/adma.202206577>.
46. Lei, H., Dong, L., Li, Y., Zhang, J., Chen, H., Wu, J., Zhang, Y., Fan, Q., Xue, B., Qin, M., et al. (2020). Stretchable hydrogels with low hysteresis and anti-fatigue fracture based on polyprotein cross-linkers. *Nat. Commun.* **11**, 4032. <https://doi.org/10.1038/s41467-020-17877-z>.
47. Xiong, X., Chen, Y., Wang, Z., Liu, H., Le, M., Lin, C., Wu, G., Wang, L., Shi, X., Jia, Y.-G., and Zhao, Y. (2023). Polymerizable rotaxane hydrogels for three-dimensional printing fabrication of wearable sensors. *Nat. Commun.* **14**, 1331. <https://doi.org/10.1038/s41467-023-36920-3>.
48. Meng, X., Qiao, Y., Do, C., Bras, W., He, C., Ke, Y., Russell, T.P., and Qiu, D. (2022). Hysteresis-Free Nanoparticle-Reinforced Hydrogels. *Adv. Mater.* **34**, 2108243. <https://doi.org/10.1002/adma.202108243>.
49. Li, W., Wang, X., Liu, Z., Zou, X., Shen, Z., Liu, D., Li, L., Guo, Y., and Yan, F. (2024). Nanoconfined polymerization limits crack propagation in hysteresis-free gels. *Nat. Mater.* **23**, 131–138. <https://doi.org/10.1038/s41563-023-01697-9>.
50. Cao, P., Wang, Y., Yang, J., Niu, S., Pan, X., Lu, W., Li, L., Xu, Y., Cui, J., Ho, G.W., and Wang, X.Q. (2024). Scalable Layered Heterogeneous Hydrogel Fibers with Strain-Induced Crystallization for Tough, Resilient, and Highly Conductive Soft Bioelectronics. *Adv. Mater.* **36**, 2409632. <https://doi.org/10.1002/adma.202409632>.
51. Zhang, G., Steck, J., Kim, J., Ahn, C.H., and Suo, Z. (2023). Hydrogels of arrested phase separation simultaneously achieve high strength and low hysteresis. *Sci. Adv.* **9**, eadh7742. <https://doi.org/10.1126/sciadv.adh7742>.
52. Petelinsek, N., and Mommer, S. (2024). Tough Hydrogels for Load-Bearing Applications. *Adv. Sci.* **11**, 2307404. <https://doi.org/10.1002/advs.202307404>.
53. Li, C., Wang, Z., Wang, Y., He, Q., Long, R., and Cai, S. (2021). Effects of network structures on the fracture of hydrogel. *Extreme Mech. Lett.* **49**, 101495. <https://doi.org/10.1016/j.eml.2021.101495>.
54. Seiffert, S. (2017). Origin of nanostructural inhomogeneity in polymer-network gels. *Polym. Chem.* **8**, 4472–4487. <https://doi.org/10.1039/C7PY01035D>.
55. Seiffert, S. (2017). Scattering perspectives on nanostructural inhomogeneity in polymer network gels. *Prog. Polym. Sci.* **66**, 1–21. <https://doi.org/10.1016/j.progpolymsci.2016.12.011>.
56. Yang, C., Yin, T., and Suo, Z. (2019). Polyacrylamide hydrogels. I. Network imperfection. *J. Mech. Phys. Solids* **131**, 43–55. <https://doi.org/10.1016/j.jmps.2019.06.018>.
57. Kim, J., Zhang, G., Shi, M., and Suo, Z. (2021). Fracture, fatigue, and friction of polymers in which entanglements greatly outnumber cross-links. *Science* **374**, 212–216. <https://doi.org/10.1126/science.abg6320>.
58. Chen, G., Zhang, Y., Li, S., Zheng, J., Yang, H., Ren, J., Zhu, C., Zhou, Y., Chen, Y., and Fu, J. (2024). Flexible Artificial Tactility with Excellent Robustness and Temperature Tolerance Based on Organohydrogel Sensor Array for Robot Motion Detection and Object Shape Recognition. *Adv. Mater.* **36**, 2408193. <https://doi.org/10.1002/adma.202408193>.
59. Zhong, M., Wang, R., Kawamoto, K., Olsen, B.D., and Johnson, J.A. (2016). Quantifying the impact of molecular defects on polymer network elasticity. *Science* **353**, 1264–1268. <https://doi.org/10.1126/science.aag0184>.
60. Han, S., Hu, Y., Wei, J., Li, S., Yang, P., Mi, H., Liu, C., and Shen, C. (2024). A Semi-Interpenetrating Poly(Ionic Liquid) Network-Driven Low Hysteresis and Transparent Hydrogel as a Self-Powered Multifunctional Sensor. *Adv. Funct. Mater.* **34**, 2401607. <https://doi.org/10.1002/adfm.202401607>.
61. Zhao, H., Hao, S., Fu, Q., Zhang, X., Meng, L., Xu, F., and Yang, J. (2022). Ultrafast Fabrication of Lignin-Encapsulated Silica Nanoparticles Reinforced Conductive Hydrogels with High Elasticity and Self-Adhesion for Strain Sensors. *Chem. Mater.* **34**, 5258–5272. <https://doi.org/10.1021/acs.chemmater.2c00934>.
62. Burla, F., Mulla, Y., Vos, B.E., Aufderhorst-Roberts, A., and Koenderink, G.H. (2019). From mechanical resilience to active material properties in biopolymer networks. *Nat. Rev. Phys.* **1**, 249–263. <https://doi.org/10.1038/s42254-019-0036-4>.
63. Wu, J., Li, P., Dong, C., Jiang, H., Bin, X., Gao, X., Qin, M., Wang, W., Bin, C., and Cao, Y. (2018). Rationally designed synthetic protein hydrogels with predictable mechanical properties. *Nat. Commun.* **9**, 620. <https://doi.org/10.1038/s41467-018-02917-6>.
64. Liu, R., Wang, H., Lu, W., Cui, L., Wang, S., Wang, Y., Chen, Q., Guan, Y., and Zhang, Y. (2021). Highly tough, stretchable and resilient hydrogels strengthened with molecular springs and their application as a wearable, flexible sensor. *Chem. Eng. J.* **415**, 128839. <https://doi.org/10.1016/j.cej.2021.128839>.

65. Li, Y., Wang, D., Wen, J., Liu, J., Zhang, D., Li, J., and Chu, H. (2021). Ultra-Stretchable, Variable Modulus, Shape Memory Multi-Purpose Low Hysteresis Hydrogel Derived from Solvent-Induced Dynamic Micelle Sea-Island Structure. *Adv. Funct. Mater.* *31*, 2011259. <https://doi.org/10.1002/adfm.202011259>.
66. Xiong, J., Wang, X., Li, L., Li, Q., Zheng, S., Liu, Z., Li, W., and Yan, F. (2024). Low-Hysteresis and High-Toughness Hydrogels Regulated by Porous Cationic Polymers: The Effect of Counteranions. *Angew. Chem. Int. Ed.* *63*, e202316375. <https://doi.org/10.1002/anie.202316375>.
67. Wang, J., Tang, F., Yao, C., and Li, L. (2023). Low Hysteresis Hydrogel Induced by Spatial Confinement. *Adv. Funct. Mater.* *33*, 2214935. <https://doi.org/10.1002/adfm.202214935>.
68. Lantz, M.A., Jarvis, S.P., Tokumoto, H., Martynski, T., Kusumi, T., Nakamura, C., and Miyake, J. (1999). Stretching the α -helix: a direct measure of the hydrogen-bond energy of a single-peptide molecule. *Chem. Phys. Lett.* *315*, 61–68. [https://doi.org/10.1016/S0009-2614\(99\)01201-4](https://doi.org/10.1016/S0009-2614(99)01201-4).
69. Liu, P., Zhang, Y., Guan, Y., and Zhang, Y. (2023). Peptide-Crosslinked, Highly Entangled Hydrogels with Excellent Mechanical Properties but Ultra-Low Solid Content. *Adv. Mater.* *35*, 2210021. <https://doi.org/10.1002/adma.202210021>.
70. Zhang, Y., Wang, Y., Guan, Y., and Zhang, Y. (2022). Peptide-enhanced tough, resilient and adhesive eutectogels for highly reliable strain/pressure sensing under extreme conditions. *Nat. Commun.* *13*, 6671. <https://doi.org/10.1038/s41467-022-34522-z>.
71. Zhang, Q., Zhang, Y., Li, W., Chen, X., Jiang, Y., Wang, B., Yao, J., Yang, Y., Zou, L., Zhao, Z., et al. (2025). Spider silk-like strong and adhesive eutectogel fibers fabricated via a continuous spinning-polymerization process. *Chem. Eng. J.* *507*, 160437. <https://doi.org/10.1016/j.cej.2025.160437>.
72. Jeon, I., Cui, J., Illeperuma, W.R.K., Aizenberg, J., and Vlassak, J.J. (2016). Extremely Stretchable and Fast Self-Healing Hydrogels. *Adv. Mater.* *28*, 4678–4683. <https://doi.org/10.1002/adma.201600480>.
73. Qu, J., Zhao, X., Liang, Y., Zhang, T., Ma, P.X., and Guo, B. (2018). Antibacterial adhesive injectable hydrogels with rapid self-healing, extensibility and compressibility as wound dressing for joints skin wound healing. *Biomaterials* *183*, 185–199. <https://doi.org/10.1016/j.biomaterials.2018.08.044>.
74. Zhao, X., Chen, X., Yuk, H., Lin, S., Liu, X., and Parada, G. (2021). Soft Materials by Design: Unconventional Polymer Networks Give Extreme Properties. *Chem. Rev.* *121*, 4309–4372. <https://doi.org/10.1021/acs.chemrev.0c01088>.
75. Liu, C., Kadono, H., Mayumi, K., Kato, K., Yokoyama, H., and Ito, K. (2017). Unusual Fracture Behavior of Slide-Ring Gels with Movable Cross-Links. *ACS Macro Lett.* *6*, 1409–1413. <https://doi.org/10.1021/acsmacrolett.7b00729>.
76. Guo, X., Li, J., Wang, J., Huang, L., Cheng, G., Zhang, Q., Zhu, H., Zhang, M., and Zhu, S. (2022). Stretchable Hydrogels with Low Hysteresis and High Fracture Toughness for Flexible Electronics. *Macromol. Rapid Commun.* *43*, 2100716. <https://doi.org/10.1002/marc.202100716>.
77. Xu, K., Shen, K., Yu, J., Yang, Y., Wei, Y., Lin, P., Zhang, Q., Xiao, C., Zhang, Y., and Cheng, Y. (2022). Ultradurable Noncovalent Cross-Linked Hydrogels with Low Hysteresis and Robust Elasticity for Flexible Electronics. *Chem. Mater.* *34*, 3311–3322. <https://doi.org/10.1021/acs.chemmater.2c00093>.
78. Guan, S., Xu, C., Dong, X., and Qi, M. (2023). A highly tough, fatigue-resistant, low hysteresis hybrid hydrogel with a hierarchical cross-linked structure for wearable strain sensors. *J. Mater. Chem. A* *11*, 15404–15415. <https://doi.org/10.1039/D3TA02584E>.
79. Li, T., Li, X., Yang, J., Sun, H., and Sun, J. (2023). Healable Ionic Conductors with Extremely Low-Hysteresis and High Mechanical Strength Enabled by Hydrophobic Domain-Locked Reversible Interactions. *Adv. Mater.* *35*, 2307990. <https://doi.org/10.1002/adma.202307990>.
80. Wang, H., Liu, B., Chen, D., Wang, Z., Wang, H., Bao, S., Zhang, P., Yang, J., and Liu, W. (2024). Low hysteresis zwitterionic supramolecular polymer ion-conductive elastomers with anti-freezing properties, high stretchability, and self-adhesion for flexible electronic devices. *Mater. Horiz.* *11*, 2628–2642. <https://doi.org/10.1039/D4MH00174E>.
81. Si, W., Liang, Y., Chen, Y., and Zhang, S. (2022). A multifunctional sustainable ionohydrogel with excellent low-hysteresis-driven mechanical performance, environmental tolerance, multimodal stimuli-responsiveness, and power generation ability for wearable electronics. *J. Mater. Chem. A* *10*, 17464–17476. <https://doi.org/10.1039/D2TA04276B>.
82. Yu, X., Zhang, H., Wang, Y., Fan, X., Li, Z., Zhang, X., and Liu, T. (2022). Highly Stretchable, Ultra-Soft, and Fast Self-Healable Conductive Hydrogels Based on Polyaniline Nanoparticles for Sensitive Flexible Sensors. *Adv. Funct. Mater.* *32*, 2204366. <https://doi.org/10.1002/adfm.202204366>.
83. Zou, J., Jing, X., Chen, Z., Wang, S.J., Hu, X.S., Feng, P.Y., and Liu, Y.J. (2023). Multifunctional Organohydrogel with Ultralow-Hysteresis, Ultrafast-Response, and Whole-Strain-Range Linearity for Self-Powered Sensors. *Adv. Funct. Mater.* *33*, 2213895. <https://doi.org/10.1002/adfm.202213895>.
84. Guo, S., Zhu, S., Qiao, Y., Feng, S., Yang, X., Kang, B., Yue, C., Zhang, Y., Li, Z., Ye, Y.N., and Zheng, Q. (2025). Ultra-Low Hysteresis Under Large Deformation Enabled by Fast Chains Relaxation in Highly Competitive Dynamic Hydrogen Bond Networks. *Adv. Sci.* *12*, e05417. <https://doi.org/10.1002/advs.202505417>.
85. Song, Z., Yang, Z., Zhang, Y., Luo, J., Cha, Y., Sui, S., and Zhang, Y. (2025). Janus adhesion hydrogels with low hysteresis and high sensitivity toward precision flexible electronics underwater. *Chem. Eng. J.* *521*, 166386. <https://doi.org/10.1016/j.cej.2025.166386>.
86. Liu, Q., Xie, M., Wang, C., Deng, M., Li, P., Yang, X., Zhao, N., Huang, C., and Zhang, X. (2024). Rapid Preparation Triggered by Visible Light for Tough Hydrogel Sensors with Low Hysteresis and High Elasticity: Mechanism, Use and Recycle-by-Design. *Small* *20*, 2311647. <https://doi.org/10.1002/sml.202311647>.
87. Wen, J., Tang, J., Ning, H., Hu, N., Zhu, Y., Gong, Y., Xu, C., Zhao, Q., Jiang, X., Hu, X., et al. (2021). Multifunctional Ionic Skin with Sensing, UV-Filtering, Water-Retaining, and Anti-Freezing Capabilities. *Adv. Funct. Mater.* *31*, 2011176. <https://doi.org/10.1002/adfm.202011176>.
88. Thoniyot, P., Tan, M.J., Karim, A.A., Young, D.J., and Loh, X.J. (2015). Nanoparticle–Hydrogel Composites: Concept, Design, and Applications of These Promising, Multi-Functional Materials. *Adv. Sci.* *2*, 1400010. <https://doi.org/10.1002/advs.201400010>.
89. Li, W., Zheng, S., Zou, X., Ren, Y., Liu, Z., Peng, W., Wang, X., Liu, D., Shen, Z., Hu, Y., et al. (2022). Tough Hydrogels with Isotropic and Unprecedented Crack Propagation Resistance. *Adv. Funct. Mater.* *32*, 2207348. <https://doi.org/10.1002/adfm.202207348>.
90. Zhou, L., Zhao, B., Liang, J., Lu, F., Yang, W., Xu, J., Zheng, J., Liu, Y., Wang, R., and Liu, Z. (2024). Low hysteresis, water retention, anti-freeze multifunctional hydrogel strain sensor for human–machine interfacing and real-time sign language translation. *Mater. Horiz.* *11*, 3856–3866. <https://doi.org/10.1039/D4MH00126E>.
91. Ko, S., Chhetry, A., Kim, D., Yoon, H., and Park, J.Y. (2022). Hysteresis-Free Double-Network Hydrogel-Based Strain Sensor for Wearable Smart Bioelectronics. *ACS Appl. Mater. Interfaces* *14*, 31363–31372. <https://doi.org/10.1021/acsmami.2c09895>.
92. Ji, D., Kim, D.-Y., Fan, Z., Lee, C.-S., and Kim, J. (2024). Hysteresis-Free, Elastic, and Tough Hydrogel with Stretch-Rate Independence and High Stability in Physiological Conditions. *Small* *20*, 2309217. <https://doi.org/10.1002/sml.202309217>.
93. Zou, J., Jing, X., Li, S., Feng, P., Chen, Y., and Liu, Y. (2024). MXene Crosslinked Hydrogels with Low Hysteresis Conferred by Sliding Tangle Island Strategy. *Small* *20*, 2401622. <https://doi.org/10.1002/sml.202401622>.

94. Zhou, Y., Shu, H., Yao, Y., Yang, X., Yu, C., and Zhong, W. (2024). An ultralow hysteresis zwitterionic hydrogel crosslinked by functionalized graphene oxide quantum dots for dual-responsive flexible wearable sensors. *Chem. Eng. J.* *483*, 149282. <https://doi.org/10.1016/j.cej.2024.149282>.
95. Lin, W.-C., Marcellan, A., Hourdet, D., and Creton, C. (2011). Effect of polymer-particle interaction on the fracture toughness of silica filled hydrogels. *Soft Matter* *7*, 6578–6582. <https://doi.org/10.1039/C1SM05420A>.
96. Fu, L., Li, L., Bian, Q., Xue, B., Jin, J., Li, J., Cao, Y., Jiang, Q., and Li, H. (2023). Cartilage-like protein hydrogels engineered via entanglement. *Nature* *618*, 740–747. <https://doi.org/10.1038/s41586-023-06037-0>.
97. Sun, H., Zhou, K., Yu, Y., Yue, X., Dai, K., Zheng, G., Liu, C., and Shen, C. (2019). Highly Stretchable, Transparent, and Bio-Friendly Strain Sensor Based on Self-Recovery Ionic-Covalent Hydrogels for Human Motion Monitoring. *Macromol. Mater. Eng.* *304*, 1900227. <https://doi.org/10.1002/mame.201900227>.
98. Wang, X., Li, N., Yin, J., Wang, X., Xu, L., Jiao, T., and Qin, Z. (2023). Interface interaction-mediated design of tough and conductive MXene-composited polymer hydrogel with high stretchability and low hysteresis for high-performance multiple sensing. *Sci. China Mater.* *66*, 272–283. <https://doi.org/10.1007/s40843-022-2105-6>.
99. Liu, Y., Tian, G., Du, Y., Shi, P., Li, N., Li, Y., Qin, Z., Jiao, T., and He, X. (2024). Highly Stretchable, Low-Hysteresis, and Adhesive TA@MXene-Composited Organohydrogels for Durable Wearable Sensors. *Adv. Funct. Mater.* *34*, 2315813. <https://doi.org/10.1002/adfm.202315813>.
100. Li, Y., Yan, J., Liu, Y., and Xie, X.-M. (2022). Super Tough and Intelligent Multibond Network Physical Hydrogels Facilitated by Ti3C2Tx MXene Nanosheets. *ACS Nano* *16*, 1567–1577. <https://doi.org/10.1021/acsnano.1c10151>.
101. Norioka, C., Inamoto, Y., Hajime, C., Kawamura, A., and Miyata, T. (2021). A universal method to easily design tough and stretchable hydrogels. *NPG Asia Mater.* *13*, 34. <https://doi.org/10.1038/s41427-021-00302-2>.
102. Maganaris, C.N., and Paul, J.P. (2000). Hysteresis measurements in intact human tendon. *J. Biomech.* *33*, 1723–1727. [https://doi.org/10.1016/S0021-9290\(00\)00130-5](https://doi.org/10.1016/S0021-9290(00)00130-5).
103. Keten, S., Xu, Z., Ihle, B., and Buehler, M.J. (2010). Nanoconfinement controls stiffness, strength and mechanical toughness of β -sheet crystals in silk. *Nat. Mater.* *9*, 359–367. <https://doi.org/10.1038/nmat2704>.
104. Liu, X., Ji, X., Zhu, R., Gu, J., and Liang, J. (2024). A Microphase-Separated Design toward an All-Round Ionic Hydrogel with Discriminable and Anti-Disturbance Multisensory Functions. *Adv. Mater.* *36*, 2309508. <https://doi.org/10.1002/adma.202309508>.
105. Gavrilov, A.A., and Potemkin, I.I. (2018). Adaptive structure of gels and microgels with sliding cross-links: enhanced softness, stretchability and permeability. *Soft Matter* *14*, 5098–5105. <https://doi.org/10.1039/C8SM00192H>.
106. Shen, Z., Zhang, Z., Zhang, N., Li, J., Zhou, P., Hu, F., Rong, Y., Lu, B., and Gu, G. (2022). High-Stretchability, Ultralow-Hysteresis Conducting Polymer Hydrogel Strain Sensors for Soft Machines. *Adv. Mater.* *34*, 2203650. <https://doi.org/10.1002/adma.202203650>.
107. Peng, Q., Chen, J., Wang, T., Peng, X., Liu, J., Wang, X., Wang, J., and Zeng, H. (2020). Recent advances in designing conductive hydrogels for flexible electronics. *InfoMat* *2*, 843–865. <https://doi.org/10.1002/inf2.12113>.
108. Liu, Y., Tao, J., Mo, Y., Bao, R., and Pan, C. (2024). Ultrasensitive Touch Sensor for Simultaneous Tactile and Slip Sensing. *Adv. Mater.* *36*, 2313857. <https://doi.org/10.1002/adma.202313857>.
109. Li, X., Wu, G., Gao, C., Bao, R., and Pan, C. (2025). Flexible Electronic Devices and Wearable Sensors Based on Liquid Metals. *MetalMat* *2*, e70000. <https://doi.org/10.1002/metm.70000>.
110. Zhao, Y., Wu, R., Hao, Y., Zhao, Y., Zhang, X., Liu, H., Zhai, W., Dai, K., Pan, C., Liu, C., and Shen, C. (2025). Eco-Friendly Multifunctional Hydrogel Sensors Enabled Sustainable and Accurate Human-Machine Interaction System. *Adv. Mater.* *37*, 2507127. <https://doi.org/10.1002/adma.202507127>.
111. Zuo, X., Zhou, Y., Hao, K., Liu, C., Yu, R., Huang, A., Wu, C., and Yang, Y. (2024). 3D Printed All-Natural Hydrogels: Flame-Retardant Materials Toward Attaining Green Sustainability. *Adv. Sci.* *11*, 2306360. <https://doi.org/10.1002/advs.202306360>.
112. Niu, Q., Huang, L., Fan, S., Yao, X., and Zhang, Y. (2024). 3D Printing Silk Fibroin/Polyacrylamide Triple-Network Composite Hydrogels with Stretchability, Conductivity, and Strain-Sensing Ability as Bionic Electronic Skins. *ACS Biomater. Sci. Eng.* *10*, 3489–3499. <https://doi.org/10.1021/acsbomaterials.4c00201>.
113. Ma, J., Zhong, J., Sun, F., Liu, B., Peng, Z., Lian, J., Wu, X., Li, L., Hao, M., and Zhang, T. (2024). Hydrogel sensors for biomedical electronics. *Chem. Eng. J.* *481*, 148317. <https://doi.org/10.1016/j.cej.2023.148317>.
114. Liu, R., Liu, Y., Fu, S., Cheng, Y., Jin, K., Ma, J., Wan, Y., and Tian, Y. (2024). Humidity Adaptive Antifreeze Hydrogel Sensor for Intelligent Control and Human-Computer Interaction. *Small* *20*, 2308092. <https://doi.org/10.1002/smll.202308092>.
115. Tao, J., Dong, M., Li, L., Wang, C., Li, J., Liu, Y., Bao, R., and Pan, C. (2020). Real-time pressure mapping smart insole system based on a controllable vertical pore dielectric layer. *Microsyst. Nanoeng.* *6*, 62. <https://doi.org/10.1038/s41378-020-0171-1>.
116. Xia, S., Song, S., and Gao, G. (2018). Robust and flexible strain sensors based on dual physically cross-linked double network hydrogels for monitoring human-motion. *Chem. Eng. J.* *354*, 817–824. <https://doi.org/10.1016/j.cej.2018.08.053>.
117. Wu, G., Li, X., Bao, R., and Pan, C. (2024). Innovations in Tactile Sensing: Microstructural Designs for Superior Flexible Sensor Performance. *Adv. Funct. Mater.* *34*, 2405722. <https://doi.org/10.1002/adfm.202405722>.
118. Xu, L., Liu, S., Zhu, L., Liu, Y., Li, N., Shi, X., Jiao, T., and Qin, Z. (2023). Hydroxypropyl methyl cellulose reinforced conducting polymer hydrogels with ultra-stretchability and low hysteresis as highly sensitive strain sensors for wearable health monitoring. *Int. J. Biol. Macromol.* *236*, 123956. <https://doi.org/10.1016/j.ijbiomac.2023.123956>.
119. Li, S., Xiao, Z., Yang, H., Zhu, C., Chen, G., Zheng, J., Ren, J., Wang, W., Cong, Y., Ali Shah, L., and Fu, J. (2024). A skin-inspired anisotropic multidimensional sensor based on low hysteresis organohydrogel with linear sensitivity and excellent robustness for directional perception. *Chem. Eng. J.* *499*, 156581. <https://doi.org/10.1016/j.cej.2024.156581>.
120. Huang, W., Wang, X., Luo, F., Zhao, X., Chen, K., and Qin, Y. (2024). Ultrastretchable, Ultralow Hysteresis, High-Toughness Hydrogel Strain Sensor for Pressure Recognition with Deep Learning. *ACS Appl. Mater. Interfaces* *16*, 49834–49844. <https://doi.org/10.1021/acsaami.4c12419>.
121. Aisyah Nurmaulia Entifar, S., Aqilla Ellenahaya Entifar, N., Fitriani Wibowo, A., Ha Kim, J., Shara br Sembiring, Y., Martino Windi Saputro, J., Kim, H.-G., Kim, J.-O., Xie, G., Oh, J., et al. (2025). Extremely-low electrical-hysteresis hydrogels for multifunctional wearable sensors and osmotic power generators. *Chem. Eng. J.* *509*, 160971. <https://doi.org/10.1016/j.cej.2025.160971>.
122. Zou, J., Jing, X., Li, S., Chen, Y., Liu, Y., Feng, P.-Y., and Peng, X.-F. (2025). Low mechanical-hysteresis conductive hydrogel conferred by chitosan bridging and MXene nanoconfined mechanism. *Carbohydr. Polym.* *348*, 122849. <https://doi.org/10.1016/j.carbpol.2024.122849>.
123. Zhao, Z., Rong, Y., Cui, P., Qin, G., Wang, H., and Huang, X. (2024). High elongation, low hysteresis, fatigue resistant gel electrolyte for supercapacitor and strain sensor. *J. Power Sources* *622*, 235307. <https://doi.org/10.1016/j.jpowsour.2024.235307>.
124. Liu, J., Chen, X., Sun, B., Guo, H., Guo, Y., Zhang, S., Tao, R., Yang, Q., and Tang, J. (2022). Stretchable strain sensor of composite hydrogels with high fatigue resistance and low hysteresis. *J. Mater. Chem. A* *10*, 25564–25574. <https://doi.org/10.1039/D2TA07447H>.

125. Shen, S., Zhang, J., Han, Y., Pu, C., Duan, Q., Huang, J., Yan, B., You, X., Lin, R., Shen, X., et al. (2023). A Core–Shell Nanoreinforced Ion-Conductive Implantable Hydrogel Bioelectronic Patch with High Sensitivity and Bioactivity for Real-Time Synchronous Heart Monitoring and Repairing. *Adv. Healthc. Mater.* **12**, 2301990. <https://doi.org/10.1002/adhm.202301990>.
126. Wang, M., Li, L., and Zhang, T. (2024). Hysteresis-free, fatigue-resistant and self-adhesive conductive hydrogel electronics towards multimodal wearable application. *Nano Energy* **126**, 109586. <https://doi.org/10.1016/j.nanoen.2024.109586>.
127. Li, X., Wu, G., Pan, C., and Bao, R. (2025). Recent progress in flexible sensors based on 2D materials. *J. Semicond.* **46**, 011607. <https://doi.org/10.1088/1674-4926/24090044>.
128. Lai, B.-Y., Lai, S.-N., Lin, H.-Y., and Wu, J.M. (2024). Silane-modified MXene/PVA hydrogel for enhanced streaming vibration potential in high-performance flexible triboelectric nanogenerators. *Nano Energy* **125**, 109554. <https://doi.org/10.1016/j.nanoen.2024.109554>.
129. Ding, Y., Guo, H., Ouyang, M., Meng, G., Chen, F., and Kuang, T. (2024). Humidity-Resistant Wearable Triboelectric Nanogenerator Utilizing a Bound-Water-Rich Zwitterionic Hydrogel With Microphase-Separated Domains. *Adv. Funct. Mater.* **35**, 2421164. <https://doi.org/10.1002/adfm.202421164>.
130. Jiang, W., Liu, J., Zhang, H., Song, D., Yu, J., Liu, Q., Chen, R., Zhu, J., and Wang, J. (2024). Low-temperature resistant hydrogel with inkjet-printed MXene on microspine surface for pressure sensing and triboelectric energy harvesting. *Chem. Eng. J.* **483**, 149117. <https://doi.org/10.1016/j.cej.2024.149117>.
131. Febriola, N.A., Singh, S., Jeong, E., and Yoon, J. (2025). Highly deformable triboelectric nanogenerators fabricated using high-dielectric elastomers and double-network ionic hydrogels for use in energy harvesting and motion sensing. *Chem. Eng. J.* **503**, 158641. <https://doi.org/10.1016/j.cej.2024.158641>.
132. Li, R., Jia, W., Wen, J., Hu, G., Tang, T., Li, X., Jiang, L., Li, M., Huang, H., and Fang, G. (2024). MXene/Zwitterionic Hydrogel Oriented Anti-freezing and High-Performance Zinc-Ion Hybrid Supercapacitor. *Adv. Funct. Mater.* **34**, 2409207. <https://doi.org/10.1002/adfm.202409207>.
133. Wu, Y., Huang, L.-B., and Pan, C. (2023). Halide perovskite-based tribovoltaic effects for self-powered sensors. *Sci. Bull.* **68**, 1849–1852. <https://doi.org/10.1016/j.scib.2023.07.042>.
134. Zhang, W., Guo, F., Mi, H., Wu, Z.-S., Ji, C., Yang, C., and Qiu, J. (2022). Kinetics-Boosted Effect Enabled by Zwitterionic Hydrogel Electrolyte for Highly Reversible Zinc Anode in Zinc-Ion Hybrid Micro-Supercapacitors. *Adv. Energy Mater.* **12**, 2202219. <https://doi.org/10.1002/aenm.202202219>.
135. Luo, N., Wang, J., Zhang, D., Zhao, Y., Wei, Y., Liu, Y., Zhang, Y., Han, S., Kong, X., and Huo, P. (2024). Inorganic nanoparticle-enhanced double-network hydrogel electrolytes for supercapacitor with superior low-temperature adaptability. *Chem. Eng. J.* **479**, 147741. <https://doi.org/10.1016/j.cej.2023.147741>.
136. Li, Q., Tian, B., Tang, G., Zhan, H., Liang, J., Guo, P., Liu, Q., and Wu, W. (2024). Multifunctional conductive hydrogels for wearable sensors and supercapacitors. *J. Mater. Chem. A* **12**, 3589–3600. <https://doi.org/10.1039/D3TA06771H>.
137. Xu, W., and Chen, A. (2024). Application of supramolecular hydrogel in supercapacitors: Opportunities and challenges. *Aggregate* **5**, e581. <https://doi.org/10.1002/agt2.581>.
138. Luo, X., Nian, Q., Dong, Q., Ruan, D., Cui, Z., Wang, Z., Xiong, B.-Q., and Ren, X. (2024). Anti-Swelling Supramolecule-Crosslinked Hydrogel Interphase for Stable Zn Metal Anodes. *Adv. Energy Mater.* **15**, 2403187. <https://doi.org/10.1002/aenm.202403187>.
139. Huang, X., Yang, N., Sun, S., Cheng, Y., and Cheng, L. (2025). Recent progress of hydrogel-based bioelectronics for mechanophysiological signal sensing. *Mater. Sci. Eng. R Rep.* **162**, 100888. <https://doi.org/10.1016/j.mser.2024.100888>.
140. He, Q., Cheng, Y., Deng, Y., Wen, F., Lai, Y., and Li, H. (2024). Conductive Hydrogel for Flexible Bioelectronic Device: Current Progress and Future Perspective. *Adv. Funct. Mater.* **34**, 2308974. <https://doi.org/10.1002/adfm.202308974>.
141. Huang, S., Liu, X., Lin, S., Glynn, C., Felix, K., Sahasrabudhe, A., Maley, C., Xu, J., Chen, W., Hong, E., et al. (2024). Control of polymers' amorphous-crystalline transition enables miniaturization and multifunctional integration for hydrogel bioelectronics. *Nat. Commun.* **15**, 3525. <https://doi.org/10.1038/s41467-024-47988-w>.
142. Jiang, L., Gan, D., Xu, C., Zhang, T., Gao, M., Xie, C., Zhang, D., and Lu, X. (2025). Polyphenol-Mediated Multifunctional Human–Machine Interface Hydrogel Electrodes in Bioelectronics. *Small Sci.* **5**, 2400362. <https://doi.org/10.1002/smsc.202400362>.
143. He, X., Liu, D., Cui, B., Huang, H., Dai, S., Pang, I., Qiao, Y., Xu, T., and Zhang, S. (2024). Extreme Hydrogel Bioelectronics. *Adv. Funct. Mater.* **34**, 2405896. <https://doi.org/10.1002/adfm.202405896>.
144. Lee, H.K., Yang, Y.J., Koirala, G.R., Oh, S., and Kim, T.-i. (2024). From lab to wearables: Innovations in multifunctional hydrogel chemistry for next-generation bioelectronic devices. *Biomaterials* **310**, 122632. <https://doi.org/10.1016/j.biomaterials.2024.122632>.
145. Sun, B., Liu, K., Wu, B., Sun, S., and Wu, P. (2024). Low-Hysteresis and Tough Ionogels via Low-Energy-Dissipating Cross-Linking. *Adv. Mater.* **36**, 2408826. <https://doi.org/10.1002/adma.202408826>.
146. Du, R., Bao, T., Zhu, T., Zhang, J., Huang, X., Jin, Q., Xin, M., Pan, L., Zhang, Q., and Jia, X. (2023). A Low-Hysteresis and Highly Stretchable Ionogel Enabled by Well Dispersed Slidable Cross-Linker for Rapid Human-Machine Interaction. *Adv. Funct. Mater.* **33**, 2212888. <https://doi.org/10.1002/adfm.202212888>.
147. Zhang, Z., Qian, L., Cheng, J., Ma, C., and Zhang, G. (2024). Neural Network-Inspired Polyurea Ionogel with Mechanical Robustness, Low Hysteresis, and High Transparency for Soft Iontronics. *Adv. Funct. Mater.* **34**, 2402115. <https://doi.org/10.1002/adfm.202402115>.
148. Li, X., Yang, X., Li, S., Lv, H., Wang, Z., Gao, Z., and Song, H. (2024). 3D Printing of Thermo-Mechano-Responsive Photoluminescent Noncovalent Cross-Linked Ionogels with High-Stretchability and Ultralow-Hysteresis for Wearable Iontronics and Anti-Counterfeiting. *Small* **20**, 2403252. <https://doi.org/10.1002/sml.202403252>.